

**Uncertainties in
modeling ozone
depletion**

I. Wohltmann et al.

This discussion paper is/has been under review for the journal Atmospheric Chemistry and Physics (ACP). Please refer to the corresponding final paper in ACP if available.

Uncertainties in modeling heterogeneous chemistry and Arctic ozone depletion in the winter 2009/2010

I. Wohltmann¹, T. Wegner², R. Müller², R. Lehmann¹, M. Rex¹, G. L. Manney^{3,4}, M. L. Santee⁵, P. Bernath^{6,7}, O. Sumińska-Ebersoldt⁸, F. Strohm², M. von Hobe², C. M. Volk⁹, E. Hösen⁹, F. Ravegnani¹⁰, A. Ulanovsky¹¹, and V. Yushkov¹¹

¹ Alfred Wegener Institute for Polar and Marine Research, Potsdam, Germany

² Institute of Energy and Climate Research – Stratosphere (IEK-7), Forschungszentrum Jülich, Jülich, Germany

³ NorthWest Research Associates, Inc., Socorro, New Mexico, USA

⁴ New Mexico Institute of Mining and Technology, Socorro, New Mexico, USA

⁵ Jet Propulsion Laboratory, California Institute of Technology, Pasadena, California, USA

⁶ University of York, York, UK

⁷ Old Dominion University, Norfolk, VA, USA

⁸ Institute of Meteorology and Climate Research, Karlsruhe Institute of Technology, Karlsruhe, Germany

⁹ University of Wuppertal, Department of Physics, Wuppertal, Germany

¹⁰ ISAC-CNR, Bologna, Italy

¹¹ Central Aerological Observatory, Dolgoprudny, Russia

Title Page

Abstract

Introduction

Conclusions

References

Tables

Figures

◀

▶

◀

▶

Back

Close

Full Screen / Esc

Printer-friendly Version

Interactive Discussion



Received: 13 September 2012 – Accepted: 19 September 2012 – Published: 5 October 2012

Correspondence to: I. Wohltmann (ingo.wohltmann@awi.de)

Published by Copernicus Publications on behalf of the European Geosciences Union.

Discussion Paper | Discussion Paper | Discussion Paper | Discussion Paper | Discussion Paper

ACPD

12, 26245–26295, 2012

Uncertainties in modeling ozone depletion

I. Wohltmann et al.

Title Page

Abstract

Introduction

Conclusions

References

Tables

Figures

⏪

⏩

◀

▶

Back

Close

Full Screen / Esc

Printer-friendly Version

Interactive Discussion



Abstract

Stratospheric chemistry and denitrification are simulated for the Arctic winter 2009/2010 with the Lagrangian Chemistry and Transport Model ATLAS. A number of sensitivity runs is used to explore the impact of uncertainties in chlorine activation and denitrification on the model results. In particular, the efficiency of chlorine activation on different types of liquid aerosol versus activation on nitric acid trihydrate clouds is examined. Additionally, the impact of changes in reaction rate coefficients, in the particle number density of polar stratospheric clouds, in supersaturation, temperature or the extent of denitrification is investigated. Results are compared to satellite measurements of MLS and ACE-FTS and to in-situ measurements onboard the Geophysica aircraft during the RECONCILE measurement campaign. It is shown that even large changes in the underlying assumptions have only a small impact on the modeled ozone loss, even though they can cause considerable differences in chemical evolution and denitrification. In addition, it is shown that chlorine activation on liquid aerosols alone is able to explain the observed magnitude and morphology of the mixing ratios of active chlorine, reservoir gases and ozone.

1 Introduction

After the discovery of the Antarctic ozone hole (Farman et al., 1985), the rapid development of a robust theory of anthropogenic ozone depletion was a great scientific achievement. Since then, many aspects of this theory have been confirmed in a great number of modeling and observational studies (e.g. Solomon, 1999; WMO, 2011). However, uncertainties in theory and observations of polar ozone depletion and limitations in modeling the complex processes in Chemistry and Transport Models (CTMs) remain an important issue. This is especially true for the microphysics and chemistry of Polar Stratospheric Clouds (PSCs) (e.g. Lowe and MacKenzie, 2008; Peter and Groöf, 2012). Here, the following uncertainties will be examined:

ACPD

12, 26245–26295, 2012

Uncertainties in modeling ozone depletion

I. Wohltmann et al.

Title Page

Abstract

Introduction

Conclusions

References

Tables

Figures

◀

▶

◀

▶

Back

Close

Full Screen / Esc

Printer-friendly Version

Interactive Discussion



Uncertainties in modeling ozone depletion

I. Wohltmann et al.

Title Page

Abstract

Introduction

Conclusions

References

Tables

Figures

◀

▶

◀

▶

Back

Close

Full Screen / Esc

Printer-friendly Version

Interactive Discussion



– In 2005, K. Drdla attracted attention with her hypothesis that the generally accepted mechanism of dominant chlorine activation on clouds composed of nitric acid trihydrate (NAT) or supercooled ternary solutions (STS) might not be necessary for efficient chlorine activation and that heterogeneous activation of chlorine reservoir species might very efficiently occur already on the cold background aerosol (e.g. Drdla, 2005; Drdla and Müller, 2012). In fact, it is largely unknown to what extent liquid aerosols contribute to chlorine activation in relation to NAT clouds in the atmosphere. A change in this ratio would have important implications for the prediction of future ozone depletion in model scenarios. Drdla's hypothesis is backed by the current low estimates of NAT number density, the required high supersaturation of HNO_3 over NAT and the large uncertainties in reaction rates on NAT, which we will discuss in detail later.

– Reaction rate coefficients on liquid aerosols and gas-surface reaction probabilities on solid cloud particles are poorly constrained. Here, we compare the parameterization of Carslaw et al. (1997) on liquid aerosols (based on laboratory studies by Hanson and Ravishankara, 1994) to the rates of Shi et al. (2001) and the parameterization of Carslaw et al. (1997) on NAT clouds (based on laboratory studies by Hanson and Ravishankara, 1993) to the alternative parameterization from the same paper based on the studies of Abbatt and Molina (1992).

– Additionally, we consider several other uncertainties, including the number density of NAT cloud particles, the required supersaturation for NAT formation, the impact of a possible temperature bias in the analysis data and the impact of denitrification on ozone depletion.

The RECONCILE project was initiated to help resolving these uncertainties and aims at a better quantitative understanding of the dynamical, chemical and microphysical processes influencing polar ozone depletion (von Hobe et al., 2012). As a part of the project, the first major measurement campaign in the Arctic winter stratosphere since

the SOLVE/THESEO (1999/2000) and VINTERSOL-EUPLEX (2002/2003) campaigns was conducted in 2009/2010.

Here, we use runs of the global Chemistry and Transport Model ATLAS to give an overview over the chemical evolution of the winter 2009/2010 and to assess the impact of the major uncertainties in the model formulation on the chemical results of the model.

Results are extensively compared to satellite observations of many trace species by the MLS instrument onboard the Aura satellite (Waters et al., 2006) and by the ACE-FTS instrument onboard the SCISAT-1 satellite (Bernath et al., 2005). Additionally, in-situ measurements onboard the Geophysica aircraft and ozone sonde ascents conducted during the campaign are used for the comparison (von Hobe et al., 2012). The Supplement includes all comparisons to measurements performed in the frame of this study. The paper shows only a representative selection.

In a related and complementary study, Wegner et al. (2012) validate the heterogeneous chemistry parameterizations with in-situ data from 2005 and 2010 and show that activation on background aerosol is sufficient to explain the measurements. In addition, they show that there is no correlation between chlorine activation and the formation of Polar Stratospheric Clouds in MLS data.

2 The model

2.1 Model overview

ATLAS is a global Chemistry and Transport Model (CTM) based on a Lagrangian (trajectory-based) approach. A detailed description of the model can be found in Wohltmann and Rex (2009) and Wohltmann et al. (2010).

Transport and chemistry in the model are driven by reanalysis data of the European Centre for Medium-Range Weather Forecasts (ECMWF). A large number of trajectories is initialized and advected with this input. Chemistry is simulated on every trajectory as in a box model.

Uncertainties in modeling ozone depletion

I. Wohltmann et al.

Title Page

Abstract

Introduction

Conclusions

References

Tables

Figures



Back

Close

Full Screen / Esc

Printer-friendly Version

Interactive Discussion



Uncertainties in modeling ozone depletion

I. Wohltmann et al.

Title Page

Abstract

Introduction

Conclusions

References

Tables

Figures

◀

▶

◀

▶

Back

Close

Full Screen / Esc

Printer-friendly Version

Interactive Discussion



An important feature of the model is the mixing algorithm (Konopka et al., 2004; Wohltmann and Rex, 2009), which simulates atmospheric mixing and diffusion based on a physical approach using properties of the wind fields (i.e. shear and strain). This approach is necessary in Lagrangian models (which, unlike Eulerian models, show no numerical diffusion), and allows for a realistic simulation of atmospheric diffusion by tuning the algorithm to observations.

The model includes a gas phase stratospheric chemistry module, heterogeneous chemistry on PSCs and a particle-based Lagrangian denitrification module. The chemistry module comprises 47 active species and more than 180 reactions. The chemistry module is updated compared to Wohltmann et al. (2010). New reactions are shown in Table 1. Br₂ is added as a new species. Absorption cross sections and rate coefficients are taken from recent JPL recommendations (Sander et al., 2011), except for the Cl₂O₂ photolysis, which is from Burkholder et al. (1990). For technical reasons, we cannot use the JPL recommendation (Papanastasiou et al., 2009), which however gives very similar results.

2.2 The heterogeneous chemistry module

The heterogeneous chemistry module includes 30 different reactions on binary and ternary solutions, nitric acid trihydrate clouds and ice clouds (see Table 2). 14 reactions are added compared to Wohltmann et al. (2010).

The existence and composition of ternary solutions is calculated according to Carslaw et al. (1995). Ternary solutions are formed only if no ice clouds exist. NAT or ice particles form if the saturation mixing ratios of HNO₃ over NAT or H₂O over ice exceed a given supersaturation. Saturation mixing ratios are calculated from the expressions in Hanson and Mauersberger (1988) for NAT and Marti and Mauersberger (1993) for ice. NAT particles are assumed to form from the ternary solution droplets (see Section 4 for a discussion). The number density of the droplets and the available H₂SO₄ is adjusted accordingly. Water ice clouds form in addition to NAT clouds if the given supersaturation of H₂O over ice is exceeded.

Uncertainties in modeling ozone depletion

I. Wohltmann et al.

Title Page

Abstract

Introduction

Conclusions

References

Tables

Figures

◀

▶

◀

▶

Back

Close

Full Screen / Esc

Printer-friendly Version

Interactive Discussion



All particle types form instantly in equilibrium and are assumed to have a constant predefined number density. A uniform particle radius and a surface area density are calculated from the number density and the amount of HNO_3 or H_2O exceeding the saturation mixing ratio for NAT or ice clouds, respectively. In a similar way, the mean radius of a size distribution is adjusted for ternary solutions. The fractions of HNO_3 , H_2O and HCl contained in the cloud particles are not available for gas phase reactions.

Technically, NAT clouds are formed before STS in the model, i.e. above the given supersaturation of HNO_3 over NAT, only NAT clouds and no ternary liquid clouds will exist, since they consume the available HNO_3 . This is probably an overestimation of NAT occurrence, since often, ternary liquids and NAT clouds are observed at the same time (Pitts et al., 2011; Peter and GrooB, 2012).

The initialization of liquid H_2SO_4 for the background aerosol has changed compared to Wohltmann et al. (2010). H_2SO_4 mixing ratios have been reduced to a maximum of 0.12 ppb to make the surface area densities of the model compare better to surface area densities inferred from SAGE II. For this purpose, we fitted the calculated vortex mean surface area densities of the reference run to the CCMVal surface area density climatology (Thomason and Peter, 2006) averaged over January to March of all years between 1997 to 2004 and latitudes north of 70°N .

Constant values for the gas-surface reaction probabilities γ on NAT and ice clouds are employed in the model, with the exception of the reactions $\text{ClONO}_2 + \text{HCl}$ and $\text{ClONO}_2 + \text{H}_2\text{O}$ on NAT (Table 2). By default, we use the parameterization scheme 1 in Carslaw et al. (1997), which is based on the laboratory studies of Hanson and Ravishankara (1993). Alternatively, the scheme 2 of Carslaw et al. (1997), which is based on the studies of Abbatt and Molina (1992), can be used. By default, the reactions $\text{ClONO}_2 + \text{HCl}$ and $\text{ClONO}_2 + \text{H}_2\text{O}$ on ternary solutions are parameterized according to Shi et al. (2001). Alternatively, the parameterization of Hanson and Ravishankara (1994) can be used. Note that Shi et al. (2001) is the current JPL recommendation (Sander et al., 2011). The parameterization of Shi et al. (2001) is valid for binary

aerosols only and is extended for ternary solutions as described in Wegner et al. (2012).

The denitrification module simulates the nucleation, transport, growth and sedimentation of a large number of PSC particles and is based on the DLAPSE model of Carslaw et al. (2002), for details see Wohltmann et al. (2010).

The model simulates two different modes of NAT particles: A small mode with particles of about 1 μm radius on which the heterogeneous reactions take place, but which do not sediment in the model, and a large mode with radii of about 10 μm (“NAT rocks”, Fahey et al., 2001) in the particle module, which does not take part in the chemistry in the model. Here, we assume that the surface area density of the NAT rocks is small enough to be negligible compared to the surface area of the small mode.

2.3 Model setup

Model runs are driven by meteorological data from the ECMWF ERA Interim reanalysis (Dee et al., 2011) on 60 model levels (6 h temporal resolution, $2^\circ \times 2^\circ$ horizontal resolution). Horizontal model resolution is approximately 150 km (see Wohltmann and Rex, 2009) and vertical resolution is 1–2 km. The runs use the hybrid pressure-potential temperature coordinate of the model, which is a pure potential temperature coordinate above 100 hPa. The vertical motion is driven by diabatic heating rates (clear sky) from ERA Interim. The lower model boundary is at 350 K potential temperature and the upper boundary at 1900 K. Mixing strength by the critical Lyapunov exponent is set to 3 d^{-1} (optimal mixing, see Wohltmann and Rex, 2009) and the mixing time step to 12 h. The runs are started on 1 November 2009 and end on 31 March 2010. Chemical species are initialized on 1 December to allow for a spin-up in the mixing. Chemical species at the lower and upper boundary are re-initialized every 12 h, as described in Wohltmann and Rex (2009).

In addition to the chemical species, two tracers are included. A passive ozone tracer is initialized with the ozone values of 1 December, but no chemistry acts on the tracer in the following. The difference between the passive ozone tracer and the chemically

Uncertainties in modeling ozone depletion

I. Wohltmann et al.

Title Page

Abstract

Introduction

Conclusions

References

Tables

Figures

◀

▶

◀

▶

Back

Close

Full Screen / Esc

Printer-friendly Version

Interactive Discussion



active ozone is then a measure for chemical ozone depletion. In an equivalent way, a passive NO_y tracer is set up by adding up all nitrogen-containing species (except for N_2O and N_2). The difference between this tracer and NO_y is then a measure for denitrification by sedimenting particles.

5 The number density of NAT particles in the reference run is set to 0.1 cm^{-3} , since this is an upper limit for the majority of measurements (e.g. Northway et al., 2002; Voigt et al., 2005; Pitts et al., 2009, 2011). For a more detailed discussion, see Drdla and Müller (2012) or Peter and Grooß (2012). The number density of ice particles is set to 0.01 cm^{-3} and the number density of the ternary solution droplets to 10 cm^{-3} .

10 A supersaturation of 10 is assumed to be necessary for the formation of the NAT particles (corresponding to about 3 K supercooling). This value is estimated from atmospheric observations (e.g. Dye et al., 1990, 1992; Pitts et al., 2007) and laboratory work (Wagner et al., 2005), for discussion see Drdla and Müller (2012) or Peter and Grooß (2012).

15 The Lagrangian particle model is used to simulate the nucleation, sedimentation, growth and evaporation of large NAT particles. Particles are formed with a nucleation rate of 7.8×10^{-6} particles per h and cm^3 (Voigt et al., 2005; Grooß et al., 2005) and an initial radius of $0.1 \mu\text{m}$, wherever the temperature is below the NAT equilibrium temperature.

20 2.4 Sensitivity runs

In addition to the reference run (REF), several sensitivity runs are carried out (Table 3):

We explore the hypotheses of Drdla and Müller with several runs that allow activation only on liquid aerosol, but not on NAT or ice clouds. A run ONLY-LIQ-TER is performed that allows activation only on liquid ternary aerosols, but with everything else unchanged in the heterogeneous chemistry module. That is, the default rates of Shi et al. (2001) are used for liquid aerosols and uptake of HNO_3 is allowed. Additionally, we perform a run ONLY-LIQ-TER-HR with activation only on liquid ternary aerosols and the reaction rates of Hanson and Ravishankara (1994) for the reactions $\text{ClONO}_2 + \text{HCl}$

Uncertainties in modeling ozone depletion

I. Wohltmann et al.

Title Page

Abstract

Introduction

Conclusions

References

Tables

Figures

◀

▶

◀

▶

Back

Close

Full Screen / Esc

Printer-friendly Version

Interactive Discussion



and $\text{ClONO}_2 + \text{H}_2\text{O}$ on liquid aerosol instead of the default rates from Shi et al. (2001). Finally, we perform a run ONLY-LIQ-BIN that allows activation only on binary aerosols (no uptake of HNO_3) and uses the rates of Shi et al. (2001). NAT clouds were switched off in the ONLY-LIQ-TER, ONLY-LIQ-TER-HR and ONLY-LIQ-BIN runs as a surrogate for using the very slow reaction rates based on Abbatt and Molina (1992) and prescribing a low NAT surface area density, as done in the “NAT, current” case of Drdla and Müller (2012).

In addition, a run ABBATT with the NAT reaction rates based on Abbatt and Molina (1992) is performed, which uses the same PSC parameterization as the reference run. This results in the same HNO_3 uptake on NAT clouds as in the reference run, but in no heterogeneous activation on NAT due to the low reaction rates. That is, it is expected that the ABBATT run shows similar activation to the ONLY-LIQ-BIN run due to the small HNO_3 uptake by liquid aerosols. In the “NAT, current” case of Drdla and Müller (2012), low surface area densities are assumed in addition. These either require very low number densities for NAT (10^{-4} cm^{-3} or lower) or gas-phase HNO_3 and NAT to be in non-equilibrium for higher NAT number densities. Since our equilibrium model always uses all available HNO_3 above the NAT saturation mixing ratio to form NAT, the results for the ABBATT run are independent of the NAT number density if the chlorine activation on the NAT clouds is negligible. However, if we had assumed non-equilibrium and higher NAT number densities to obtain the low NAT surface area density, uptake of the additional gas-phase HNO_3 by liquids would have produced results similar to the ONLY-LIQ-TER run.

A run with a global temperature offset of -1 K is used to study the sensitivity to temperature changes (MINUS-ONE-KELVIN). Reaction rates for liquid aerosols show a large sensitivity to temperature changes. A typical order of magnitude for differences between reanalysis temperatures and observations is 1 K . E.g., Wegner et al. (2012) show that there is a 1.5 K bias between ERA Interim and Geophysica measurements in 2005.

Uncertainties in modeling ozone depletion

I. Wohltmann et al.

[Title Page](#)[Abstract](#)[Introduction](#)[Conclusions](#)[References](#)[Tables](#)[Figures](#)[⏪](#)[⏩](#)[◀](#)[▶](#)[Back](#)[Close](#)[Full Screen / Esc](#)[Printer-friendly Version](#)[Interactive Discussion](#)

A run with the denitrification by sedimentation of large NAT particles switched off (NO-DENITRI), and a run with the nucleation rate of “NAT rocks” multiplied by 10 (MORE-DENITRI) explore the sensitivity of the results to the simulated extent of denitrification.

Several runs examine the sensitivity of the results to microphysical parameters, which are still not well known (Peter and Grooß, 2012): a run with no supersaturation required for the formation of NAT particles (NO-SUPERSAT), a run with a supersaturation of 30 (5 K supercooling, MORE-SUPERSAT), a run with the number density of NAT particles set to 1 cm^{-3} (REF \times 10, MORE-NATPART), and a run with the number density of NAT particles set to 0.01 cm^{-3} (REF/10, LESS-NATPART).

We also tested the importance of ice clouds for chlorine activation. The reference run uses a supersaturation of 4, which effectively switches ice clouds off. A run with no supersaturation (not shown) shows identical results, which suggests that ice clouds play no role for the activation in this winter, even though they were observed in amounts unusual for the Arctic (Pitts et al., 2011).

Several of the sensitivity runs deliberately use unrealistic conditions (e.g. the number density in the MORE-NATPART run or no denitrification in the NO-DENITRI run) to show that even unrealistic changes do not cause large deviations from the reference run.

Chemistry is only calculated north of 30° N latitude for the sensitivity runs to save computing time. South of 30° N , the mixing ratios are constantly re-initialized with the results of the reference run.

2.5 Chemical initialization

H_2O , N_2O , HCl , O_3 , CO and HNO_3 are initialized from all measurements of the MLS instrument on the Aura satellite performed during 1 December 2009 (Waters et al., 2006; Livesey et al., 2011, Version 3.3 data). The location of the air masses sampled by the satellite measurements at the initialization time of the model (00:00 UTC) is

Uncertainties in modeling ozone depletion

I. Wohltmann et al.

Title Page

Abstract

Introduction

Conclusions

References

Tables

Figures

⏪

⏩

◀

▶

Back

Close

Full Screen / Esc

Printer-friendly Version

Interactive Discussion



determined by calculating short backward trajectories from the time and location of the satellite measurement to the model initialization time.

CH_4 is initialized from a monthly mean HALOE climatology (mean of the years 1991–2002) as a function of equivalent latitude and pressure (Grooß and Russell III, 2005).

All values are multiplied by 1.066 to account for the trend in CH_4 (e.g. WMO, 2011). NO_x is initialized from the monthly mean HALOE data set by putting all NO_x into NO_2 .

ClONO_2 is calculated as the difference between Cl_y and HCl . Cl_y is taken from a Cl_y - N_2O tracer-tracer correlation from ER-2 aircraft and Triple balloon data (Grooß et al., 2002). The reference run and all sensitivity runs show a systematic and persistent bias compared to measurements with this initialization. That is, less ozone depletion than observed (about 10 DU in the column), less chlorine activation (up to 0.4 ppb less ClO in sunlit conditions) and more HCl (up to 0.5 ppb). A run with ClONO_2 taken from measurements of the MIPAS instrument onboard the Envisat satellite on 1 December, with the profiles retrieved by the Oxford L2 processor MORSE (<http://www.atm.ox.ac.uk/group/mipas/>) gave similar results (not shown in the following). Hence, we increase ClONO_2 by 10 %:

$$\text{ClONO}_2 = 1.1(\text{Cl}_y - \text{HCl}) \quad (1)$$

HCl is decreased by the same amount to conserve Cl_y :

$$\text{HCl}_{\text{new}} = \text{HCl} - 0.1 \text{ClONO}_2 \quad (2)$$

This leads to a better agreement between measurements and the reference run and all sensitivity runs. However, there is still a moderate underestimation of chlorine activation in all runs. It seems not unlikely that the bias is indeed caused by small differences in the partitioning between HCl and ClONO_2 , since small changes in the partitioning have a rather large effect on the results of the model runs and the changes that define the sensitivity runs do not reduce the systematic bias in HCl .

BrONO_2 is assumed to contain all Br_y , which is taken from a Br_y - CH_4 relationship from ER-2 aircraft and Triple balloon data in Grooß et al. (2002), with Br_y deduced from

Uncertainties in modeling ozone depletion

I. Wohltmann et al.

Title Page

Abstract

Introduction

Conclusions

References

Tables

Figures

◀

▶

◀

▶

Back

Close

Full Screen / Esc

Printer-friendly Version

Interactive Discussion



the organic source gases. The obtained Br_y is scaled by a constant factor to give maximum Br_y values of 19.9 ppt to agree with Differential Optical Absorption Spectroscopy (DOAS) measurements of BrO (Dorf et al., 2008).

CFCs and Halons (which have no relevant effects on the time scales considered in this study) are initialized as in Wohltmann et al. (2010).

3 Model results and comparison to observations

3.1 Meteorological situation

In the context of the Arctic stratospheric winters of the last decades, the winter of 2009/2010 was one of the more dynamically disturbed and warm winters. However, the polar vortex experienced an exceptionally cold phase for a short period during January 2010, when the vortex was relatively isolated and stable for several weeks (see also Dörnbrack et al., 2012, for more details).

The polar vortex formed in the early days of December 2009 at the 475 K level, on which we will concentrate here. Already during the formation phase of the vortex, a wave 2 event starting on 6 December split the vortex into two parts by 10 December. The two parts reunited about 10 days later, but mixed in some extra-vortex air. The first temperatures below the NAT equilibrium temperature were observed around 17 December. For the next four weeks, the vortex remained relatively stable and isolated. Temperatures remained low and reached the ice frost point on a synoptic scale around 15 January.

Starting a few days later, the vortex was gradually displaced to Siberia by a developing major warming. The last temperatures below the ice frost point were observed around 25 January. The development of the major warming culminated at the end of January and beginning of February. The warming event was accompanied by a pronounced rise of the temperatures to more than 200 K almost everywhere in the vortex by mid February. Finally, the vortex was torn into two parts on 11 February. These two

Uncertainties in modeling ozone depletion

I. Wohltmann et al.

Title Page

Abstract

Introduction

Conclusions

References

Tables

Figures

⏪

⏩

◀

▶

Back

Close

Full Screen / Esc

Printer-friendly Version

Interactive Discussion



parts (one small part located over Canada and a larger part over Siberia) remained surprisingly stable until 1 March, when they were united again. The reunited vortex then remained stable for some weeks and finally dissipated.

Observations by the CALIPSO satellite (Pitts et al., 2011) show only patchy STS/NAT mixtures with low NAT number densities up to the end of December. The first half of January was characterized by widespread STS/NAT mixtures with higher NAT number densities. From 15 to 21 January, synoptic scale ice clouds were observed, which is rare in the Arctic. The last PSC period, which lasted to the end of January, was dominated by STS clouds.

3.2 Chlorine activation

Figure 1 shows the vortex-averaged active chlorine ($\text{ClO}_x = \text{ClO} + 2\text{Cl}_2\text{O}_2$) of the reference run as a function of time and potential temperature. Compared to colder winters, the period of chlorine activation was relatively short. Chlorine activation set in at the end of December and ClO_x reached maximum values of about 2.1 ppb in the second half of January, when the lowest temperatures were observed. Chlorine was deactivated very quickly during early February, when the major warming set in.

The comparison of the simulated ClO of the reference run with vortex means of satellite measurements of the MLS instrument (Fig. 2, top row) shows that the general morphology is matched well by the model. However, a quantitative comparison of the modeled and observed vortex average of ClO is difficult. The distribution of the local times of the observations differs from that of the model results, and these differences in temporal sampling could give rise to differences in their respective vortex average values.

For a quantitative comparison, we calculated backward trajectories starting at selected satellite measurements and ending at the time of the last model output before the measurement. Then, we initialized a chemical box model (based on the same set of reactions as the full model) with the model data and calculated the evolution of the species forward in time to obtain values to compare with the satellite measurements

Uncertainties in modeling ozone depletion

I. Wohltmann et al.

Title Page

Abstract

Introduction

Conclusions

References

Tables

Figures



Back

Close

Full Screen / Esc

Printer-friendly Version

Interactive Discussion



(see Wohltmann et al., 2010, for details). Figure 3 shows the results for 27 January at 46 hPa, the results for additional dates can be found in Sect. 4 (Fig. S17) in the Supplement. The comparison indicates an underestimation of ClO by the model (typically 0.1–0.4 ppb). This is consistent with an overestimation of the vortex-averaged HCl of about 0.3 ppb by the model compared to MLS in the same time period and altitude range (see next section). Hence, the underestimation is more likely caused by an underestimation of ClO_x than by uncertainties in the partitioning between ClO and Cl₂O₂.

The ClO measurements of MLS are corrected as described in Livesey et al. (2011) for the negative bias mentioned in Santee et al. (2008). The remaining uncertainties are around 0.1 ppb and cannot explain the differences between model results and measurements.

However, ClO measurements of the HALOX instrument (von Hobe et al., 2005; Sumińska-Ebersoldt et al., 2012) onboard the Geophysica agree well with the model results (see Sect. 1, Fig. S7, in the Supplement). But note that these measurements were obtained at about 430 K, where ClO mixing ratios are smaller. The reason for the large discrepancy between the model and the profile measured on 30 January is unclear.

The left panel of Fig. 4 shows the vortex mean chlorine activation in all sensitivity runs and the reference run on 18 January 2010, when all runs show strong activation. The small plots on the right show the same data, but now only a single or two sensitivity runs per plot for clarity. The runs show considerable differences in the absolute amount of chlorine activation at the peak of the profile, ranging from 1.7 ppb for the ONLY-LIQ-BIN run to 2.3 ppb for the MINUS-ONE-KELVIN and NO-SUPERSAT runs. The reference run shows an activation of 2.1 ppb. The differences between the peak mixing ratios in the sensitivity runs are within 30 %.

The runs with activation only on liquid ternary aerosols (ONLY-LIQ-TER and ONLY-LIQ-TER-HR) show almost identical results to the reference run (2.1 ppb and 2.0 ppb, respectively). The shape and also the magnitude of the profiles show that the activation on liquid aerosols alone is efficient enough to explain a large part of the observed

Uncertainties in modeling ozone depletion

I. Wohltmann et al.

Title Page

Abstract

Introduction

Conclusions

References

Tables

Figures

◀

▶

◀

▶

Back

Close

Full Screen / Esc

Printer-friendly Version

Interactive Discussion



chlorine activation and ozone depletion. The Shi et al. (2001) reaction rates in the ONLY-LIQ-TER run cause only a small increase of 0.1 ppb in the chlorine activation compared to the rates of Hanson and Ravishankara (1994) in the ONLY-LIQ-TER-HR run.

Chlorine activation in the reference run is almost identical to the ONLY-LIQ-TER run and the MORE-SUPERSAT run (which shows 2.0 ppb). This suggests that the supersaturation in the reference run and the MORE-SUPERSAT run was so high that almost no NAT clouds formed. Notable differences between the runs with and without NAT clouds can only be achieved by decreasing the supersaturation and increasing the NAT number densities.

The degree of chlorine activation is moderately larger in the runs with no supersaturation (NO-SUPERSAT) and more NAT particles (MORE-NATPART) due to the increased mean surface area density (2.3 ppb and 2.2 ppb, respectively). The opposite is true for the LESS-NATPART run (2.0 ppb). That is, even large changes in supersaturation and number density, which reach the limits of realistic values in the atmosphere, do only cause changes in chlorine activation in the 10 % range.

The impact of changes in the denitrification on ClO_x is small on 18 January in the model. Larger differences occur later in winter, when sunlight returns and the deactivation is hindered due to missing HNO_3 and NO_x . This can be seen clearly in the comparison of the ClO_x values of the NO-DENITRI run and the reference run in Sect. 6 (Fig. S30) in the Supplement. The NO-DENITRI shows lower ClO_x values since deactivation into ClONO_2 is enhanced compared to the reference run. On 18 January, the NO-DENITRI run shows slightly higher ClO_x values since more NO_x is available to regenerate ClONO_2 , which in turn is needed for the $\text{HCl} + \text{ClONO}_2$ heterogeneous reaction.

The MINUS-ONE-KELVIN run shows increased chlorine activation (2.3 ppb) due to the increased occurrence of polar stratospheric clouds and due to the stronger denitrification caused by the lower temperatures.

Uncertainties in modeling ozone depletion

I. Wohltmann et al.

Title Page

Abstract

Introduction

Conclusions

References

Tables

Figures

⏪

⏩

◀

▶

Back

Close

Full Screen / Esc

Printer-friendly Version

Interactive Discussion



The ONLY-LIQ-BIN run shows the lowest activation of all sensitivity runs (1.7 ppb) due to the missing uptake of HNO_3 into the droplets and the decreased surface area density. But still, the results are of similar magnitude and are able to explain a large part of the observed chlorine activation and subsequent ozone depletion. The ABBATT run shows results similar to the ONLY-LIQ-BIN run (1.9 ppb). This is because HNO_3 is depleted from the gas-phase by the NAT clouds, but the reaction rates of Abbatt and Molina (1992) are very low.

It is difficult to decide between the runs with NAT and liquid aerosol and the runs with only liquid aerosol based on the comparisons between the model runs and the comparison of the model to measured species for this winter. However, our results show that it is likely that liquid aerosols play an important role in the activation of chlorine, since NAT clouds are of second importance for the activation for current estimates of NAT number density and supersaturation.

Unfortunately, there are no usable measurements of Cl_2O_2 for this winter so far, thus no comparison with measured ClO_x is possible.

3.3 Reservoir gases

The evolution of the modeled HCl in the reference run compares well to the observations of MLS morphologically (Fig. 2, 2nd row). However, HCl is overestimated in the model by about 0.3 ppb in the regions where HCl is depleted by reactions on PSCs.

Figure 5 shows vortex mean HCl profiles on 18 January for all sensitivity runs. It is obvious that the overestimation below 550 K is common to almost all sensitivity runs. A possible reason for the discrepancy could be that the reference initialization still underestimates the real ClONO_2 amount. That would hinder the activation of chlorine by the heterogeneous reaction $\text{ClONO}_2 + \text{HCl}$ once that ClONO_2 had been completely consumed. Further activation would only continue after reformation of ClONO_2 by photolysis of HNO_3 followed by the reaction $\text{NO}_2 + \text{ClO}$.

Uncertainties in modeling ozone depletion

I. Wohltmann et al.

Title Page

Abstract

Introduction

Conclusions

References

Tables

Figures

◀

▶

◀

▶

Back

Close

Full Screen / Esc

Printer-friendly Version

Interactive Discussion



Uncertainties in modeling ozone depletion

I. Wohltmann et al.

Title Page

Abstract

Introduction

Conclusions

References

Tables

Figures

◀

▶

◀

▶

Back

Close

Full Screen / Esc

Printer-friendly Version

Interactive Discussion



There are other possible reasons for the discrepancies in HCl and ClO, e.g. a high temperature bias in the ERA Interim reanalysis. A global change of the temperature by -1 K in the MINUS-ONE-KELVIN run explains a large part of the discrepancy.

The good agreement between the NO-SUPERSAT run and the observations shows that it cannot be completely excluded that NAT clouds play a greater role in relation to liquid clouds in reality than in our reference run, which shows almost no NAT PSCs. However, the vortex-wide formation of NAT clouds directly below the NAT equilibrium temperature is not supported by observations.

Figure 6 shows vortex mean ClONO₂ profiles, which all show very low values below about 525 K, indicating that most available ClONO₂ is used up in all sensitivity runs. Above 600 K, ClONO₂ is not depleted. Figure S19 in Sect. 5 of the supplement shows that active chlorine is first transformed into ClONO₂ starting in February, which is expected under Arctic conditions (e.g. Müller et al., 1994).

Measurements of ClONO₂ for this winter were made by the ACE-FTS instrument (Bernath et al., 2005). Since ACE-FTS is a solar occultation instrument, measurements are more sparse than for the MLS instrument and are only available for the second half of the winter. In Fig. 7, we show some selected profiles of ClONO₂ and HCl measured inside the vortex on different days in comparison with the model (version 3.0 data, more species can be found in Sect. 3, Figs. S14–S16, in the Supplement). The agreement of the simulated and observed ClONO₂ is quite satisfactory below about 600 K. The ACE measurements of HCl basically confirm the results of the comparison with MLS data.

On 24 January, there was also a balloon ascent of the MIPAS-B instrument, which measured ClO, HCl and ClONO₂, but which we did not use here (Wetzel et al., 2012). Unfortunately, no instrument measures all of the important chlorine species at the same time (HCl, ClONO₂, ClO and Cl₂O₂), so that no definitive statements about the agreement of the chlorine loading and the partitioning between active chlorine and reservoir gases in measurements and model can be made.

3.4 Ozone loss

Figure 8 shows the vortex-averaged ozone loss as a function of time and potential temperature for the reference run. The largest loss rates are observed in the first half of February, shortly after the highest ClO_x values. After the warming, ozone loss continues until the end of the model run in March at a slower pace. Even though the vortex splits into two parts and is subject to considerable mixing, ozone depleted air remains clearly visible until the end of March in the model. Maximum ozone loss values of 1.4 ppm are reached in the layer between 594 K and 655 K inside the vortex by the end of the winter (30 March).

Figure 9 shows the loss profiles for the reference run and all sensitivity runs on 30 March. The differences between the sensitivity runs are within 30% (0.2 ppm). The potential temperature layer with the largest absolute differences between sensitivity runs is 471 K to 507 K. Ozone loss values are between 0.78 ppm and 0.95 ppm in this layer. Ozone loss is only slightly underestimated compared to MLS in this altitude range. Above about 600 K, NO_x -induced loss begins to dominate (note the decrease in ClO_x in Fig. 1), but this region only plays a relatively small role for the column. Here, most runs agree well, since the effects of heterogeneous chemistry begin to decrease. The MINUS-ONE-KELVIN run shows lower ozone loss here, since the NO_x cycle is more effective at higher temperatures. The maximum ozone loss in the model is underestimated compared to the MLS loss of 1.6 ppm.

Figure 10 shows the corresponding loss in the ozone column for the reference run and all sensitivity runs. The column loss in the reference run on 30 March amounts to 77 DU over the complete simulated column and to 58 DU below 600 K (better comparable to results of methods that deduce ozone loss from sonde observations, like the vortex-average method, which typically yield no results above 600 K). The simulated loss is only moderate compared to the possible range of the cumulative winter ozone losses observed in the last decades of up to 130 DU (update of Fig. 3 from Rex et al., 2006 up to and including the winter 2010/2011, Manney et al., 2011). The column loss

Uncertainties in modeling ozone depletion

I. Wohltmann et al.

Title Page

Abstract

Introduction

Conclusions

References

Tables

Figures



Back

Close

Full Screen / Esc

Printer-friendly Version

Interactive Discussion



at the end of the winter differs only by a maximum of 7 DU between the sensitivity runs (less than 10 %), showing that even large changes in the underlying assumptions on heterogeneous chemistry have only a relatively small impact on the modeled column ozone loss.

5 The differences of the sensitivity runs are to some extent sensitive to the exact procedure of averaging. In particular, taking 1 March as the ending date for the columns would give larger differences (up to 15 %), since after 1 March, the differences between the sensitivity runs and the reference run in ozone depletion decrease (see the difference of ozone loss between the sensitivity runs and the reference run in Sect. 6 in
10 the Supplement, which peak around 1 March). The decrease is probably caused by our vortex definition, which includes more and more mid-latitude air, since the vortex shrinks faster than we assume.

Likewise, calculating partial columns only up to 600 K also increases the percentage (up to 13 % on 30 March), since most of the differences in the sensitivity runs occur
15 below 600 K. Combining both effects gives differences of up to 20 %.

Comparison of vortex-averaged model ozone to MLS measurements shows a slight overestimation of ozone by the model (Fig. 2, 5th row), in line with the results for HCl and ClO of the last subsection. Accordingly, the column ozone loss of 82 DU obtained from MLS by subtracting the passive ozone tracer of the model from the MLS ozone
20 measurements is slightly larger than the modeled loss in most sensitivity runs (see Fig. 10). The NO-SUPERSAT run shows the best agreement, with a column loss of 81 DU at the end of March.

Measurements from ozone sondes and from the FOZAN instrument onboard the Geophysica (Ulanovsky et al., 2001) generally show a good agreement with the simulated ozone and also roughly confirm the simulated ozone loss (see Sect. 1, Fig. S8,
25 and Sect. 2, Fig. S13, in the Supplement).

Uncertainties in modeling ozone depletion

I. Wohltmann et al.

[Title Page](#)[Abstract](#)[Introduction](#)[Conclusions](#)[References](#)[Tables](#)[Figures](#)[⏪](#)[⏩](#)[◀](#)[▶](#)[Back](#)[Close](#)[Full Screen / Esc](#)[Printer-friendly Version](#)[Interactive Discussion](#)

3.5 Denitrification

Although the vortex was relatively disturbed (Dörnbrack et al., 2012), pronounced denitrification was simulated by the model in the reference run (Fig. 11). Denitrification set in at the beginning of January in the model with the low temperatures and reached maximum values of 7.5 ppb in the second half of January. The air remained denitrified until the end of the model run in March. Below the denitrified layer, a renitrified layer with values of up to 3.3 ppb is simulated.

Figure 12 shows NO_y (left panel) and HNO_3 (right panel) for the reference run and the relevant sensitivity runs on 2 February 2010. 2 February is around the peak of denitrification, but on a day with no uptake of HNO_3 by PSCs in the model, which would complicate the comparison. In addition, the CALIPSO satellite instrument shows no PSCs on this day (Pitts et al., 2011). Note that the passive NO_y tracer is identical to the modeled NO_y of the NO-DENITRI run (red line), i.e. the difference between the red line and any other line quantifies the denitrification. On this day, the reference run (and all other runs using the nucleation rate of the reference run except for the MINUS-ONE-KELVIN run) shows a denitrification of 7.3 ppb and a renitrification of 3.0 ppb, while the MORE-DENITRI run (nucleation rate multiplied by 10) shows 8.8 ppb denitrification and 3.9 ppb renitrification. The MINUS-ONE-KELVIN run shows more denitrification than the reference run since the lower temperatures lead to larger areas below the NAT equilibrium temperature and a faster particle growth.

Comparison with vortex-averaged observations of HNO_3 by MLS (e.g. for 2 February in the right panel) shows that the runs with the standard nucleation rate of the reference run usually show the best agreement with the measurements. The run with no denitrification is clearly not compatible with the measurements. The MORE-DENITRI run and the MINUS-ONE-KELVIN run often show lower values than the measurements.

The comparison of the time series of the vortex-averaged HNO_3 of the reference run to MLS measurements in Fig. 2 shows that mixing ratios are typically somewhat

Uncertainties in modeling ozone depletion

I. Wohltmann et al.

Title Page

Abstract

Introduction

Conclusions

References

Tables

Figures

⏪

⏩

◀

▶

Back

Close

Full Screen / Esc

Printer-friendly Version

Interactive Discussion



underestimated by the model (by less than 2 ppb), hinting at a small overestimation of the denitrification by sedimenting particles in the model in the reference run.

3.6 Long-lived tracers

A proper simulation of transport and mixing is a prerequisite for a model simulation of high quality. In addition, it excludes transport as a source of differences between model and measurement and allows attribution of the differences to e.g. the initialization or chemistry scheme. A large number of long-lived tracers was measured on the Geophysica flights by the HAGAR instrument (Volk et al., 2000). We will concentrate on N_2O and CH_4 measurements since all tracers basically allow the same conclusions and N_2O was additionally measured by MLS.

The flights generally show excellent agreement between model results and measurements, indicating no major problems (see Sect. 1, Figs. S9 and S10, in the Supplement). This is supported by the good agreement between model and MLS measurements up to February. Figure 2 shows an overestimation of N_2O by the model compared to MLS of up to 20 ppb between 20 to 25 km in February and March. There are two possible reasons for this: either an underestimation of diabatic descent in the vortex or an overestimation of the in-mixing of air rich in N_2O from outside the vortex.

Differences in heating rates and mixing between model and reality can cause discrepancies between measurements and model. E.g., an overestimation of mixing across the vortex edge would cause lower chlorine values and less ozone loss. It is difficult to quantify how large these effects are, since that would require knowledge about the correct mixing and heating rates.

4 Discussion

CALIPSO satellite measurements indicate that both STS and NAT clouds were ubiquitous in the Arctic vortex in the winter 2009/2010 (Pitts et al., 2011), with number den-

Uncertainties in modeling ozone depletion

I. Wohltmann et al.

Title Page

Abstract

Introduction

Conclusions

References

Tables

Figures

◀

▶

◀

▶

Back

Close

Full Screen / Esc

Printer-friendly Version

Interactive Discussion



sities in a broad range from 0.001 cm^{-3} to 0.1 cm^{-3} and even higher. In comparison to the other three Arctic winters observed by CALIPSO since 2006/2007, an enhanced number of high density ($> 0.1 \text{ cm}^{-3}$) STS/NAT mixture clouds was observed. A peculiarity of this winter was the widespread existence of synoptic-scale ice clouds, which were rarely observed in other Arctic winters by CALIPSO.

CALIPSO observed NAT clouds in significant quantities in this winter. Nevertheless, the runs with activation only or mainly on liquid aerosols (ONLY-LIQ-TER, ONLY-LIQ-TER-HR, ONLY-LIQ-BIN, ABBATT, MORE-SUPERSAT) show that assuming activation on liquid aerosols only is able to explain the observed magnitude and morphology of the mixing ratios of active chlorine, reservoir gases and ozone. STS clouds were observed virtually during the complete period where PSC formation was possible. In addition, the onset of chlorine activation in late December was dominated by clouds with a very low NAT number density (Pitts et al., 2011). A definitive assessment of how important activation on NAT is compared to activation on liquid aerosols is not possible with our results, since the results for the runs with and without NAT clouds are very similar. Notable differences can only be achieved by increasing the NAT number density and decreasing supersaturation. But even then, the results for the runs with and without NAT clouds are of the similar magnitude.

Based on the information from the laboratory studies alone, it is not possible to decide a priori whether the reaction rates of Abbatt and Molina (1992) or Hanson and Ravishankara (1993) on NAT clouds are closer to reality (Carslaw et al., 1997). In addition, due to the small amount of NAT clouds that form in the reference run and the ABBATT run, both runs give relatively similar results. A set of model runs that were performed in preparation of this study and which use a NAT number density of 1 cm^{-3} and a supersaturation of 4 shows that chlorine activation would be relatively small with the low ABBATT rates, if at the same time NAT clouds in appreciable amounts existed: The uptake of HNO_3 by NAT clouds would impede the uptake of HNO_3 by binary aerosols and keep their surface area low, while at the same time the NAT clouds would virtually not take part in the activation of chlorine. NAT clouds were clearly observed in

Uncertainties in modeling ozone depletion

I. Wohltmann et al.

[Title Page](#)[Abstract](#)[Introduction](#)[Conclusions](#)[References](#)[Tables](#)[Figures](#)[⏪](#)[⏩](#)[◀](#)[▶](#)[Back](#)[Close](#)[Full Screen / Esc](#)[Printer-friendly Version](#)[Interactive Discussion](#)

significant quantities in this winter, but if our model runs favor the rates of Hanson and Ravishankara (1993) over those of Abbatt and Molina (1992) depends on their surface area relative to the liquid clouds, which is not well known.

Further, it is not easy to distinguish between the rates of Shi et al. (2001) or Hanson and Ravishankara (1994) for liquid aerosols in the model. At least in our model runs for the winter 2009/2010, the change between the rates does not have a great impact on the results.

Our model assumes that NAT clouds are formed from STS droplets. There are considerable theoretical problems with this approach and the formation pathways for NAT are uncertain (Lowe and MacKenzie, 2008; Peter and Grooß, 2012). A possible alternative would be the nucleation of NAT on ice (Lowe and MacKenzie, 2008; Peter and Grooß, 2012). But on the other hand, NAT PSCs have clearly been observed without the prior formation of ice clouds (Voigt et al., 2005; Pitts et al., 2011). In particular, this is also the case for the winter 2009/2010 (Pitts et al., 2011). An inclusion of the ice mechanism into the model would produce less NAT clouds than the current mechanism if only synoptic scale clouds are considered, but could be modified by assuming temperature fluctuations by mountain waves. Another alternative would be heterogenous nucleation on e.g. meteoric material (Lowe and MacKenzie, 2008; Peter and Grooß, 2012). That could be modelled by using the current algorithm, but by switching off the correction for STS number density. This would give very similar results to the original mechanism in the model.

The weak dependence of the results on the number density of NAT particles is not too surprising. If a given constant amount of HNO_3 is distributed on a variable number N of particles, a simple calculation shows that the corresponding surface area is proportional to $N^{1/3}$. That is, increasing the number density by a factor of 10 increases the surface area only by a factor of $10^{1/3} \approx 2$.

While the results are quite insensitive to NAT number density, other factors can still cause large discrepancies between model and reality. Important reasons are the unavoidable simplification and idealization when implementing a heterogeneous chem-

Uncertainties in modeling ozone depletion

I. Wohltmann et al.

[Title Page](#)[Abstract](#)[Introduction](#)[Conclusions](#)[References](#)[Tables](#)[Figures](#)[⏪](#)[⏩](#)[◀](#)[▶](#)[Back](#)[Close](#)[Full Screen / Esc](#)[Printer-friendly Version](#)[Interactive Discussion](#)

istry and microphysics module and insufficient constraints by theory and observations. E.g., the model assumes an immediate equilibrium, while in reality, the formation and evaporation of cloud particles is a complex non-equilibrium process. This is true in particular for NAT particles, e.g. the time required to condense 50 % of available HNO_3 in the gas-phase to NAT particles at a concentration of 10^{-3} cm^{-3} is several days (Fig. 3 in Drdla and Müller, 2012). In addition, a spatially and temporally constant number density is assumed for NAT, STS and ice, and all particles are assumed to have the same size. In reality, complex mixtures of different particle types, different number densities and different size distributions exist depending on the environmental conditions, air mass history and species concentrations. However, measurements are scarce and the exact formation pathways of cloud particles are still not clear (Lowe and MacKenzie, 2008; Peter and Groß, 2012). That makes it difficult to constrain the module sufficiently by observations and theory. In addition, the module has to work fast and reliably under all environmental conditions that the model produces.

Our study is somewhat hampered by the fact that there is a persistent bias in all sensitivity runs. All runs show less active chlorine, more reservoir gases and less ozone loss than the observations. However, we believe that the relative changes between the runs still provide valuable information that is not affected by the bias. There are several possible factors that could easily explain the bias (a high temperature bias in the analysis, a systematic error in the ClONO_2 initialization, or a bias in the heating rates or mixing across the vortex edge in the analysis). However, which explanation or combination of explanations is correct is not possible to determine with the available information.

Fortunately, there is a simple reason why all these uncertainties are of secondary importance in the end: Even large changes in the underlying assumptions have only a surprisingly small impact on the modeled column ozone loss on 30 March, which differs by less than 10 % between our sensitivity runs (the percentage increases to 20 % by choosing 1 March as the end date and only a partial column below 600 K). The same is true for the differences in ClO_x , which are of the same order of magnitude,

Uncertainties in modeling ozone depletion

I. Wohltmann et al.

[Title Page](#)[Abstract](#)[Introduction](#)[Conclusions](#)[References](#)[Tables](#)[Figures](#)[⏪](#)[⏩](#)[◀](#)[▶](#)[Back](#)[Close](#)[Full Screen / Esc](#)[Printer-friendly Version](#)[Interactive Discussion](#)

but somewhat larger (up to 30 % on 18 January). Since it can be expected that ozone loss is roughly linear in ClO_x (Harris et al., 2010), the differences in ozone loss are well explained by the differences in ClO_x .

There may be several reasons why the sensitivity of ozone loss to the changes seems to be even smaller than the sensitivity of ClO_x to the changes: First, our vortex definition reduces the differences in ozone depletion between the sensitivity runs in late March, since more and more mid-latitude air is included in the average. Another reason is that the exact timing and altitude dependence of the activation are not important as long as the extent of the chlorine activation is the same in the end. Harris et al. (2010) demonstrate that several processes offset each other, e.g. the altitude dependence of the reaction rates is offset by the altitude dependence of Cl_y and the initially higher ozone loss rates in case of late activation are offset by faster deactivation. Figure 13 illustrates this very convincingly. The figure shows the mean ClO_x of the winter versus the column ozone loss on 1 March for all sensitivity runs. There is an almost perfect linear relationship between the mean chlorine activation and the column ozone loss.

5 Conclusions

We performed sensitivity runs for the Arctic winter 2009/2010 with the Lagrangian Chemistry and Transport Model ATLAS to explore the impact of uncertainties in chlorine activation and denitrification on the model results, with a particular focus on microphysics and chemistry on polar stratospheric clouds. Our main findings are:

- Even (unrealistically) large changes in the underlying assumptions have only a small impact on the modeled ozone loss. Changes in column ozone loss stayed below 10 % in our sensitivity runs. This shows that ozone loss is a robust quantity with regard to changes in the microphysical and chemical assumptions.

Uncertainties in modeling ozone depletion

I. Wohltmann et al.

Title Page

Abstract

Introduction

Conclusions

References

Tables

Figures

◀

▶

◀

▶

Back

Close

Full Screen / Esc

Printer-friendly Version

Interactive Discussion



Uncertainties in modeling ozone depletion

I. Wohltmann et al.

Title Page

Abstract

Introduction

Conclusions

References

Tables

Figures

◀

▶

◀

▶

Back

Close

Full Screen / Esc

Printer-friendly Version

Interactive Discussion



- Chlorine activation on liquid aerosols alone is sufficient to explain the observed magnitude and morphology of the mixing ratios of active chlorine, reservoir gases and ozone.
- This is even true for binary aerosols (no uptake of HNO_3 from the gas-phase allowed in the model). However, the runs with ternary aerosols agree better with the observations.
- No decision between the reaction rates of Shi et al. (2001) or Hanson and Ravishankara (1994) for liquid aerosols is possible from our results. The change between the rates only has a minor impact on the results.
- The same is true for the rates of Abbatt and Molina (1992) or Hanson and Ravishankara (1993) on NAT. However, one of the sensitivity runs with the rates of Abbatt and Molina (1992) indicates that chlorine activation would be relatively small with these rates, if at the same time NAT clouds in appreciable amounts existed. This is however not the case with our default values for supersaturation and number density.
- The timing and altitude dependence of the chlorine activation are not important in the model as long as the extent of the chlorine activation (ClO_x mixing ratio averaged over winter and all altitudes) is the same.

Our results are confirmed by the findings of Drdla and Müller (2012) and Wegner et al. (2012). Wegner et al. (2012) show that there is no interannual correlation between the depletion of HCl and the formation of NAT or STS clouds and that binary aerosol is sufficient to explain the observed chlorine activation for several trajectory case studies in 2005 and 2010.

Supplementary material related to this article is available online at:

<http://www.atmos-chem-phys-discuss.net/12/26245/2012/acpd-12-26245-2012-supplement.pdf>.

Acknowledgements. We thank ECMWF for providing reanalysis data, Nathaniel Livesey and the MLS science team at JPL for their support, the ACE team for providing ACE-FTS data, and Anu Dudhia and the University of Oxford for the MIPAS data. Work at the Jet Propulsion Laboratory, California Institute of Technology, was done under contract with the National Aeronautics and Space Administration. The Atmospheric Chemistry Experiment (ACE) mission is funded mainly by the Canadian Space Agency. Work at AWI, FZ Jülich and University of Wuppertal was supported by the EC DG research through the RECONCILE project (RECONCILE-226365-FP7-ENV-2008-1) and work at AWI was additionally supported by the SHIVA project (SHIVA-226224-FP7-ENV-2008-1).

References

- Abbat, J. P. D. and Molina, M. J.: Heterogeneous interactions of ClONO₂ and HCl on nitric acid trihydrate at 202 K, *J. Phys. Chem.*, 96, 7674–7679, 1992. 26248, 26251, 26254, 26261, 26267, 26268, 26271, 26280, 26281
- Bernath, P. F., McElroy, C. T., Abrams, M. C., Boone, C. D., Butler, M., Camy-Peyret, C., Carleer, M., Clerbaux, C., Coheur, P.-F., Colin, R., DeCola, P., DeMazière, M., Drummond, J. R., Dufour, D., Evans, W. F. J., Fast, H., Fussen, D., Gilbert, K., Jennings, D. E., Llewellyn, E. J., Lowe, R. P., Mahieu, E., McConnell, J. C., McHugh, M., McLeod, S. D., Michaud, R., Midwinter, C., Nassar, R., Nichitiu, F., Nowlan, C., Rinsland, C. P., Rochon, Y. J., Rowlands, N., Semeniuk, K., Simon, P., Skelton, R., Sloan, J. J., Soucy, M.-A., Strong, K., Tremblay, P., Turnbull, D., Walker, K. A., Walkty, I., Wardle, D. A., Wehrle, V., Zander, R., and Zou, J.: Atmospheric Chemistry Experiment (ACE): Mission overview, *Geophys. Res. Lett.*, 32, L15S01, doi:10.1029/2005GL022386, 2005. 26249, 26262
- Burkholder, J. B., Orlando, J. J., and Howard, C. J.: Ultraviolet absorption cross sections of chlorine oxide (Cl₂O₂) between 210 and 410 nm, *J. Phys. Chem.*, 94, 687–695, 1990. 26250
- Carlsaw, K., Peter, T., and Müller, R.: Uncertainties in reactive uptake coefficients for solid stratospheric particles – 2. Effect on ozone depletion, *Geophys. Res. Lett.*, 24, 1747–1750, 1997. 26248, 26251, 26267
- Carlsaw, K. S., Luo, B., and Peter, T.: An analytical expression for the composition of aqueous HNO₃-H₂SO₄ stratospheric aerosols including gas phase removal of HNO₃, *Geophys. Res. Lett.*, 22, 1877–1880, 1995. 26250

Uncertainties in modeling ozone depletion

I. Wohltmann et al.

Title Page

Abstract

Introduction

Conclusions

References

Tables

Figures

◀

▶

◀

▶

Back

Close

Full Screen / Esc

Printer-friendly Version

Interactive Discussion



Uncertainties in modeling ozone depletion

I. Wohltmann et al.

Title Page

Abstract

Introduction

Conclusions

References

Tables

Figures

◀

▶

◀

▶

Back

Close

Full Screen / Esc

Printer-friendly Version

Interactive Discussion



Carslaw, K. S., Kettleborough, J. A., Northway, M. J., Davies, S., Gao, R.-S., Fahey, D. W., Baumgardner, D. G., Chipperfield, M. P., and Kleinböhl, A.: A vortex-scale simulation of the growth and sedimentation of large nitric acid hydrate particles, *J. Geophys. Res.*, 107, 8300, doi:10.1029/2001JD000467, 2002. 26252

5 Dee, D. P., Uppala, S. M., Simmons, A. J., Berrisford, P., Poli, P., Kobayashi, S., Andrae, U., Balmaseda, M. A., Balsamo, G., Bauer, P., Bechtold, P., Beljaars, A. C. M., van de Berg, L., Bidlot, J., Bormann, N., Delsol, C., Dragani, R., Fuentes, M., Geer, A. J., Haimberger, L., Healy, S. B., Hersbach, H., Hólm, E. V., Isaksen, L., Kållberg, P., Köhler, M., Matricardi, M., McNally, A. P., Monge-Sanz, B. M., Morcrette, J.-J., Park, B.-K., Peubey, C., de Rosnay, P.,
10 Tavolato, C., Thépaut, J.-N., and Vitart, F.: The ERA-Interim reanalysis: configuration and performance of the data assimilation system, *Q. J. Roy. Meteor. Soc.*, 137, 553–597, 2011. 26252

Dorf, M., Butz, A., Camy-Peyret, C., Chipperfield, M. P., Kritten, L., and Pfeilsticker, K.: Bromine in the tropical troposphere and stratosphere as derived from balloon-borne BrO observations, *Atmos. Chem. Phys.*, 8, 7265–7271, doi:10.5194/acp-8-7265-2008, 2008. 26257

Dörnbrack, A., Pitts, M. C., Poole, L. R., Orsolini, Y. J., Nishii, K., and Nakamura, H.: The 2009–2010 Arctic stratospheric winter – general evolution, mountain waves and predictability of an operational weather forecast model, *Atmos. Chem. Phys.*, 12, 3659–3675, doi:10.5194/acp-12-3659-2012, 2012. 26257, 26265

20 Drdla, K.: Temperature threshold for polar stratospheric ozone, *EOS Trans. AGU*, 86, Fall Meet., Abstract A31D-03, 2005. 26248

Drdla, K. and Müller, R.: Temperature thresholds for chlorine activation and ozone loss in the polar stratosphere, *Ann. Geophys.*, 30, 1055–1073, 2012, <http://www.ann-geophys.net/30/1055/2012/>. 26248, 26253, 26254, 26269, 26271

25 Dye, J. E., Gandrud, B. W., Baumgardner, D., Chan, K. R., Ferry, G. V., Loewenstein, M., Kelly, K. K., and Wilson, J. C.: Observed particle evolution in the polar stratospheric cloud of January 24, 1989, *Geophys. Res. Lett.*, 17, 413–416, 1990. 26253

Dye, J. E., Baumgardner, D., Gandrud, B. W., Kawa, S. R., Kelly, K. K., Loewenstein, M., Ferry, G. V., Chan, K. R., and Gary, B. L.: Particle size distributions in Arctic polar stratospheric clouds, growth and freezing of sulfuric acid droplets, and implications for cloud formation, *J. Geophys. Res.*, 97, 8015–8034, 1992. 26253

30 Fahey, D. W., Gao, R. S., Carslaw, K. S., Kettleborough, J., Popp, P. J., Northway, M. J., Holecek, J. C., Ciciora, S. C., McLaughlin, R. J., Thompson, T. L., Winkler, R. H., Baumgardner,

Uncertainties in modeling ozone depletion

I. Wohltmann et al.

Title Page

Abstract

Introduction

Conclusions

References

Tables

Figures

◀

▶

◀

▶

Back

Close

Full Screen / Esc

Printer-friendly Version

Interactive Discussion



D. G., Gandrud, B., Wennberg, P. O., Dhaniyala, S., McKinney, K., Peter, T., Salawitch, R. J., Bui, T. P., Elkins, J. W., Webster, C. R., Atlas, E. L., Jost, H., Wilson, J. C., Herman, R. L., Kleinböhl, A., and von König, M.: The detection of large HNO₃-containing particles in the winter Arctic stratosphere, *Science*, 291, 1026–1031, 2001. 26252

5 Farman, J. C., Gardiner, B. G., and Shanklin, J. D.: Large losses of total ozone in Antarctica reveal seasonal ClO_x/NO_x interaction, *Nature*, 315, 207–210, 1985. 26247

Grooß, J.-U. and Russell III, J. M.: Technical note: A stratospheric climatology for O₃, H₂O, CH₄, NO_x, HCl and HF derived from HALOE measurements, *Atmos. Chem. Phys.*, 5, 2797–2807, 2005,

10 <http://www.atmos-chem-phys.net/5/2797/2005/>. 26256

Grooß, J.-U., Günther, G., Konopka, P., Müller, R., McKenna, D. S., Stroh, F., Vogel, B., Engel, A., Müller, M., Hoppel, K., Bevilacqua, R., Richard, E., Webster, C. R., Elkins, J. W., Hurst, D. F., Romashkin, P. A., and Baumgardner, D. G.: Simulation of ozone depletion in spring 2000 with the Chemical Lagrangian Model of the Stratosphere (CLaMS), *J. Geophys. Res.*, 107, 8295, doi:10.1029/2001JD000456, 2002. 26256

15 Grooß, J.-U., Günther, G., Müller, R., Konopka, P., Bausch, S., Schlager, H., Voigt, C., Volk, C., and Toon, G. C.: Simulation of denitrification and ozone loss for the Arctic winter 2002/2003, *Atmos. Chem. Phys.*, 5, 1437–1448, doi:10.5194/acp-5-1437-2005, 2005. 26253

Hanson, D. and Mauersberger, K.: Laboratory studies of the nitric acid trihydrate: Implications for the south polar stratosphere, *Geophys. Res. Lett.*, 15, 855–858, 1988. 26250

20 Hanson, D. R. and Ravishankara, A. R.: Reaction of ClONO₂ with HCl on NAT, NAD and frozen sulfuric acid and hydrolysis of N₂O₅ and ClONO₂ on frozen sulfuric acid, *J. Geophys. Res.*, 98, 22931–22936, 1993. 26248, 26251, 26267, 26268, 26271, 26280

Hanson, D. R. and Ravishankara, A. R.: Reactive uptake of ClONO₂ onto sulfuric acid due to reaction with HCl and H₂O, *J. Phys. Chem.*, 98, 5728–5735, 1994. 26248, 26251, 26253, 26260, 26268, 26271, 26280, 26281

25 Hanson, D. R., Ravishankara, A. R., and Solomon, S.: Heterogeneous reactions in sulfuric acid aerosols: A framework for model calculations, *J. Geophys. Res.*, 99, 3615–3629, 1994. 26280

30 Hanson, D. R., Ravishankara, A. R., and Lovejoy, E. R.: Reaction of BrONO₂ with H₂O on submicron sulfuric acid aerosol and the implications for the lower stratosphere, *J. Geophys. Res.*, 101, 9063–9069, 1996. 26280

Uncertainties in modeling ozone depletion

I. Wohltmann et al.

Title Page

Abstract

Introduction

Conclusions

References

Tables

Figures

◀

▶

◀

▶

Back

Close

Full Screen / Esc

Printer-friendly Version

Interactive Discussion



Harris, N. R. P., Lehmann, R., Rex, M., and von der Gathen, P.: A closer look at Arctic ozone loss and polar stratospheric clouds, *Atmos. Chem. Phys.*, 10, 8499–8510, doi:10.5194/acp-10-8499-2010, 2010. 26270

5 Konopka, P., Steinhorst, H.-M., Grooß, J.-U., Günther, G., Müller, R., Elkins, J. W., Jost, H.-J., Richard, E., Schmidt, U., Toon, G., and McKenna, D. S.: Mixing and ozone loss in the 1999–2000 Arctic vortex: Simulations with the three-dimensional Chemical Lagrangian Model of the Stratosphere (CLaMS), *J. Geophys. Res.*, 109, D02315, doi:10.1029/2003JD003792, 2004. 26250

10 Livesey, N. J., Read, W. G., Froidevaux, L., Lambert, A., Manney, G. L., Pumphrey, H. C., Santee, M. L., Schwartz, M. J., Wang, S., Cofeld, R. E., Cuddy, D. T., Fuller, R. A., Jarnot, R. F., Jiang, J. H., Knosp, B. W., Stek, P. C., Wagner, P. A., and Wu, D. L.: Version 3.3 Level 2 data quality and description document, JPL D-33509, <http://mls.jpl.nasa.gov>, 2011. 26255, 26259

15 Lowe, D. and MacKenzie, A. R.: Polar stratospheric cloud microphysics and chemistry, *J. Atmos. Solar-Terr. Phys.*, 70, 13–40, 2008. 26247, 26268, 26269

Manney, G. L., Santee, M. L., Rex, M., Livesey, N. J., Pitts, M. C., Veefkind, P., Nash, E. R., Wohltmann, I., Lehmann, R., Froidevaux, L., Poole, L. R., Schoeberl, M. R., Haffner, D. P., Davies, J., Dorokhov, V., Gernandt, H., Johnson, B., Kivi, R., Kyrö, E., Larsen, N., Levelt, P. F., Makshtas, A., McElroy, C. T., Nakajima, H., and Parrondo, M. C.: Unprecedented Arctic ozone loss in 2011, *Nature*, 478, 469–475, 2011. 26263

20 Marti, J. and Mauersberger, K.: A survey and new measurements of ice vapor pressure at temperatures between 170 and 250 K, *Geophys. Res. Lett.*, 20, 363–366, 1993. 26250

Müller, R., Peter, T., Crutzen, P. J., Oelhaf, H., Adrian, G. P., von Clarmann, T., Wegner, A., Schmidt, U., and Lary, D.: Chlorine chemistry and the potential for ozone depletion in the Arctic stratosphere in the winter of 1991/92, *Geophys. Res. Lett.*, 21, 1427–1430, 1994. 26262

25 Nash, E. R., Newman, P. A., Rosenfield, J. E., and Schoeberl, M. R.: An objective determination of the polar vortex using Ertel's potential vorticity, *J. Geophys. Res.*, 101, 9471–9478, 1996. 26282

30 Northway, M. J., Gao, R. S., Popp, P. J., Holecek, J. C., Fahey, D. W., Carslaw, K. S., Tolbert, M. A., Lait, L. R., Dhaniyala, S., Flagan, R. C., Wennberg, P. O., Mahoney, M. J., Herman, R. L., Toon, G. C., and Bui, T. P.: An analysis of large HNO₃-containing particles sampled

Uncertainties in modeling ozone depletion

I. Wohltmann et al.

Title Page

Abstract

Introduction

Conclusions

References

Tables

Figures

◀

▶

◀

▶

Back

Close

Full Screen / Esc

Printer-friendly Version

Interactive Discussion



in the Arctic stratosphere during the winter of 1999/2000, *J. Geophys. Res.*, 107, 8298, doi:10.1029/2001JD001079, 2002. 26253

Papanastasiou, D. K., Papadimitriou, V. C., Fahey, D. W., and Burkholder, J. B.: UV absorption spectrum of the ClO dimer (Cl₂O₂) between 200 and 420 nm, *J. Phys. Chem. A*, 113, 13711–13726, 2009. 26250

Peter, T. and Grooß, J.-U.: Polar Stratospheric Clouds and Sulfate Aerosol Particles: Microphysics, Denitrification and Heterogeneous Chemistry, in: *Stratospheric Ozone Depletion and Climate Change*, chap. 4, 108–144, RSC Publishing, 2012. 26247, 26251, 26253, 26255, 26268, 26269

Pitts, M. C., Thomason, L. W., Poole, L. R., and Winker, D. M.: Characterization of Polar Stratospheric Clouds with spaceborne lidar: CALIPSO and the 2006 Antarctic season, *Atmos. Chem. Phys.*, 7, 5207–5228, doi:10.5194/acp-7-5207-2007, 2007. 26253

Pitts, M. C., Poole, L. R., and Thomason, L. W.: CALIPSO polar stratospheric cloud observations: second-generation detection algorithm and composition discrimination, *Atmos. Chem. Phys.*, 9, 7577–7589, 2009, <http://www.atmos-chem-phys.net/9/7577/2009/>. 26253

Pitts, M. C., Poole, L. R., Dörnbrack, A., and Thomason, L. W.: The 2009–2010 Arctic polar stratospheric cloud season: a CALIPSO perspective, *Atmos. Chem. Phys.*, 11, 2161–2177, doi:10.5194/acp-11-2161-2011, 2011. 26251, 26253, 26255, 26258, 26265, 26266, 26267, 26268

Rex, M., Salawitch, R. J., Deckelmann, H., von der Gathen, P., Harris, N. R. P., Chipperfield, M. P., Naujokat, B., Reimer, E., Allaart, M., Andersen, S. B., Bevilacqua, R., Braathen, G. O., Claude, H., Davies, J., De Backer, H., Dier, H., Dorokhov, V., Fast, H., Gerding, M., Godin-Beekmann, S., Hoppel, K., Johnson, B., Kyrö, E., Litynska, Z., Moore, D., Nakane, H., Par-rondo, M. C., Risley Jr., A. D., Skrivankova, P., Stübi, R., Viatte, P., Yushkov, V., and Zerefos, C.: Arctic winter 2005: Implications for stratospheric ozone loss and climate change, *Geophys. Res. Lett.*, 33, L23808, doi:10.1029/2006GL026731, 2006. 26263

Sander, S. P., Abbatt, J., Barker, J. R., Burkholder, J. B., Friedl, R. R., Golden, D. M., Huie, R. E., Kolb, C. E., Kurylo, M. J., Moortgat, G. K., Orkin, V. L., and Wine, P. H.: Chemical kinetics and photochemical data for use in atmospheric studies, Evaluation Number 17, JPL Publication 10-06, Jet Propulsion Laboratory, California Institute of Technology, Pasadena, CA, USA, <http://jpldataeval.jpl.nasa.gov>, 2011. 26250, 26251

Uncertainties in modeling ozone depletion

I. Wohltmann et al.

Title Page

Abstract

Introduction

Conclusions

References

Tables

Figures

◀

▶

◀

▶

Back

Close

Full Screen / Esc

Printer-friendly Version

Interactive Discussion



- Santee, M. L., Lambert, A., Read, W. G., Livesey, N. J., Manney, G. L., Cofield, R. E., Cuddy, D. T., Daffer, W. H., Drouin, B. J., Froidevaux, L., Fuller, R. A., Jarnot, R. F., Knosp, B. W., Perun, V. S., Snyder, W. V., Stek, P. C., Thurstans, R. P., Wagner, P. A., Waters, J. W., Connor, B., Urban, J., Murtagh, D., Ricaud, P., Barret, B., Kleinböhl, A., Kuttippurath, J., Küllmann, H., von Hobe, M., Toon, G. C., and Stachnik, R. A.: Validation of the Aura Microwave Limb Sounder CIO measurements, *J. Geophys. Res.*, 113, D15S22, doi:10.1029/2007JD008762, 2008. 26259
- Shi, Q., Jayne, J. T., Kolb, C. E., Worsnop, D. R., and Davidovits, P.: Kinetic model for reaction of ClONO₂ with H₂O and HCl and HOCl with HCl in sulfuric acid solutions, *J. Geophys. Res.*, 106, 24259–24274, 2001. 26248, 26251, 26253, 26254, 26260, 26268, 26271, 26280
- Solomon, S.: Stratospheric ozone depletion: A review of concepts and history, *Rev. Geophys.*, 37, 275–316, 1999. 26247
- Sumińska-Ebersoldt, O., Lehmann, R., Wegner, T., Grooß, J.-U., Hösen, E., Weigel, R., Frey, W., Griessbach, S., Mitev, V., Emde, C., Volk, C. M., Borrmann, S., Rex, M., Stroh, F., and von Hobe, M.: ClOOCl photolysis at high solar zenith angles: analysis of the RECONCILE self-match flight, *Atmos. Chem. Phys.*, 12, 1353–1365, doi:10.5194/acp-12-1353-2012, 2012. 26259
- Thomason, L. and Peter, T.: Assessment of Stratospheric Aerosol Properties, SPARC Report No. 4, WMO/TD-No. 1295, <http://www.sparc-climate.org>, 2006. 26251
- Ulanovsky, A. E., Yushkov, V. A., Sitnikov, N. M., and Ravegnani, F.: The FOZAN-II Fast-Response Chemiluminescent Airborne Ozone Analyzer, *Inst. Exp. Tech.*, 44, 249–256, 2001. 26264
- Voigt, C., Schlager, H., Luo, B. P., Dörnbrack, A., Roiger, A., Stock, P., Curtius, J., Vössing, H., Borrmann, S., Davies, S., Konopka, P., Schiller, C., Shur, G., and Peter, T.: Nitric Acid Trihydrate (NAT) formation at low NAT supersaturation in Polar Stratospheric Clouds (PSCs), *Atmos. Chem. Phys.*, 5, 1371–1380, doi:10.5194/acp-5-1371-2005, 2005. 26253, 26268
- Volk, C., Riediger, O., Strunk, M., Schmidt, U., Ravegnani, F., Ulanovsky, A., and Rudakovand, V.: In situ tracer measurements in the tropical tropopause region during APE-THESEO, *Eur. Comm. Air Pollut. Res. Report 73*, 2000. 26266
- von Hobe, M., Grooß, J.-U., Müller, R., Hrechanny, S., Winkler, U., and Stroh, F.: A re-evaluation of the ClO/Cl₂O₂ equilibrium constant based on stratospheric in-situ observations, *Atmos. Chem. Phys.*, 5, 693–702, doi:10.5194/acp-5-693-2005, 2005. 26259

Uncertainties in modeling ozone depletion

I. Wohltmann et al.

Title Page

Abstract

Introduction

Conclusions

References

Tables

Figures

◀

▶

◀

▶

Back

Close

Full Screen / Esc

Printer-friendly Version

Interactive Discussion



von Hobe, M. et al.: Reconciliation of essential process parameters for an enhanced predictability of Arctic stratospheric ozone loss and its climate interactions, to be submitted to Atmos. Chem. Phys., 2012. 26248, 26249

Wagner, R., Möhler, O., Saathoff, H., Stetzer, O., and Schurath, U.: Infrared spectrum of Nitric Acid Dihydrate: Influence of particle shape, J. Phys. Chem. A, 109, 2572–2581, 2005. 26253

Waters, J. W., Froidevaux, L., Harwood, R. S., Jarnot, R. F., Pickett, H. M., Read, W. G., Siegel, P. H., Coeld, R. E., Filipiak, M. J., Flower, D. A., Holden, J. R., Lau, G. K., Livesey, N. J., Manney, G. L., Pumphrey, H. C., Santee, M. L., Wu, D. L., Cuddy, D. T., Lay, R. R., Loo, M. S., Perun, V. S., Schwartz, M. J., Stek, P. C., Thurstans, R. P., Chandra, K. M., Chavez, M. C., Chen, G.-S., Boyles, M. A., Chudasama, B. V., Dodge, R., Fuller, R. A., Girard, M. A., Jiang, J. H., Jiang, Y., Knosp, B. W., LaBelle, R. C., Lam, J. C., Lee, K. A., Miller, D., Oswald, J. E., Patel, N. C., Pukala, D. M., Quintero, O., Scaff, D. M., Snyder, W. V., Tope, M. C., Wagner, P. A., and Walch, M. J.: The Earth Observing System Microwave Limb Sounder (EOS MLS) on the Aura satellite, IEEE Trans. Geosci. Remote Sens., 44, 1075–1092, 2006. 26249, 26255

Wegner, T., Groöß, J.-U., von Hobe, M., Stroh, F., Sumińska-Ebersoldt, O., Volk, C. M., Hösen, E., Mitev, V., Shur, G., and Müller, R.: Chlorine activation on stratospheric aerosols: uncertainties in parameterizations and surface area, Atmos. Chem. Phys. Discuss., 12, 20561–20591, doi:10.5194/acpd-12-20561-2012, 2012. 26249, 26252, 26254, 26271

Wetzel, G., Oelhaf, H., Kirner, O., Friedl-Vallon, F., Ruhnke, R., Ebersoldt, A., Kleinert, A., Maucher, G., Nordmeyer, H., and Orphal, J.: Diurnal variations of reactive chlorine and nitrogen oxides observed by MIPAS-B inside the January 2010 Arctic vortex, Atmos. Chem. Phys., 12, 6581–6592, doi:10.5194/acp-12-6581-2012, 2012. 26262

WMO: World Meteorological Organization (WMO) / United Nations Environment Programme (UNEP), Scientific assessment of ozone depletion: 2010, Global Ozone Research and Monitoring Project – Report No. 52, 2011. 26247, 26256

Wohltmann, I. and Rex, M.: The Lagrangian chemistry and transport model ATLAS: validation of advective transport and mixing, Geosci. Model Dev., 2, doi:10.5194/gmd-2-153-2009, 153–173, 2009. 26249, 26250, 26252

Wohltmann, I., Lehmann, R., and Rex, M.: The Lagrangian chemistry and transport model ATLAS: simulation and validation of stratospheric chemistry and ozone loss in the winter 1999/2000, Geosci. Model Dev., 3, 585–601, doi:10.5194/gmd-3-585-2010, 2010. 26249, 26250, 26251, 26252, 26257, 26259, 26279

Uncertainties in modeling ozone depletion

I. Wohltmann et al.

Table 1. List of new gas-phase and photolysis reactions compared to Wohltmann et al. (2010).

Reaction	
$\text{Br}_2+h\nu$	$\rightarrow 2\text{Br}$
$\text{ClO}+\text{ClO}$	$\rightarrow 2\text{Cl}+\text{O}_2$
$\text{O}+\text{HOBr}$	$\rightarrow \text{OH}+\text{BrO}$
$\text{BrO}+\text{BrO}$	$\rightarrow \text{Br}_2+\text{O}_2$
Br_2+OH	$\rightarrow \text{HOBr}+\text{Br}$
$\text{Cl}_2\text{O}_2+\text{OH}$	$\rightarrow \text{HOCl}+\text{Cl}+\text{O}_2$

[Title Page](#)[Abstract](#)[Introduction](#)[Conclusions](#)[References](#)[Tables](#)[Figures](#)[I ◀](#)[▶ I](#)[◀](#)[▶](#)[Back](#)[Close](#)[Full Screen / Esc](#)[Printer-friendly Version](#)[Interactive Discussion](#)

Uncertainties in modeling ozone depletion

I. Wohltmann et al.

Table 2. List of heterogeneous reactions included in the model. The cloud types on which the reactions take place are indicated (STS = supercooled ternary solution, NAT = nitric acid trihydrate). The first column shows parameterizations for reaction rate coefficients. The last two columns give gas-surface reaction probabilities γ or parameterizations for γ . Parameterizations are indicated by HR94 = Hanson and Ravishankara (1994) and Hanson et al. (1994), Shi = Shi et al. (2001), HR93 = Hanson and Ravishankara (1993), AM92 = Abbatt and Molina (1992), H96 = Hanson et al. (1996).

Reaction	STS	γ NAT	γ Ice
$\text{ClONO}_2 + \text{H}_2\text{O} \rightarrow \text{HOCl} + \text{HNO}_3$	HR94/Shi	HR93/AM92	0.3
$\text{ClONO}_2 + \text{HCl} \rightarrow \text{Cl}_2 + \text{HNO}_3$	HR94/Shi	HR93/AM92	0.3
$\text{N}_2\text{O}_5 + \text{H}_2\text{O} \rightarrow \text{HNO}_3 + \text{HNO}_3$	HR94	0.0006	0.02
$\text{N}_2\text{O}_5 + \text{HCl} \rightarrow \text{ClONO}_2 + \text{HNO}_3$	–	0.003	0.03
$\text{HOCl} + \text{HCl} \rightarrow \text{Cl}_2 + \text{H}_2\text{O}$	HR94/Shi	0.1	0.2
$\text{BrONO}_2 + \text{H}_2\text{O} \rightarrow \text{HOBr} + \text{HNO}_3$	H96	0.006	0.3
$\text{HOBr} + \text{HCl} \rightarrow \text{BrCl} + \text{H}_2\text{O}$	HR94	0.1	0.3
$\text{ClONO}_2 + \text{HBr} \rightarrow \text{BrCl} + \text{HNO}_3$	–	0.3	0.3
$\text{BrONO}_2 + \text{HCl} \rightarrow \text{BrCl} + \text{HNO}_3$	–	–	0.3
$\text{HOCl} + \text{HBr} \rightarrow \text{BrCl} + \text{H}_2\text{O}$	HR94	0.1	0.3
$\text{HOBr} + \text{HBr} \rightarrow \text{Br}_2 + \text{H}_2\text{O}$	HR94	0.1	0.1
$\text{BrONO}_2 + \text{HBr} \rightarrow 2\text{Br} + \text{HNO}_3$	–	–	0.1

Title Page

Abstract

Introduction

Conclusions

References

Tables

Figures

◀

▶

◀

▶

Back

Close

Full Screen / Esc

Printer-friendly Version

Interactive Discussion



Uncertainties in modeling ozone depletion

I. Wohltmann et al.

Title Page

Abstract

Introduction

Conclusions

References

Tables

Figures

◀

▶

◀

▶

Back

Close

Full Screen / Esc

Printer-friendly Version

Interactive Discussion



Table 3. Sensitivity runs.

Name	Description
REF	Reference run
ONLY-LIQ-TER	Activation only on ternary solutions (No NAT or ice clouds)
ONLY-LIQ-TER-HR	As above, but with the reaction rates of Hanson and Ravishankara (1994) for ternary solutions
ONLY-LIQ-BIN	Activation only on binary aerosols (no uptake of HNO ₃)
ABBATT	Reaction rates of Abbatt and Molina (1992) for NAT
MINUS-ONE-KELVIN	Global temperature offset of –1K
NO-DENITRI	No denitrification by sedimenting particles
MORE-DENITRI	Increased nucleation rate of NAT rocks (REF × 10)
NO-SUPERSAT	No supersaturation of HNO ₃ over NAT
MORE-SUPERSAT	Supersaturation of HNO ₃ over NAT of 30 (5 K supercooling)
LESS-NATPART	Number density of NAT particles of 0.01 cm ⁻³ (REF/10)
MORE-NATPART	Number density of NAT particles of 1 cm ⁻³ (REF × 10)

Uncertainties in modeling ozone depletion

I. Wohltmann et al.

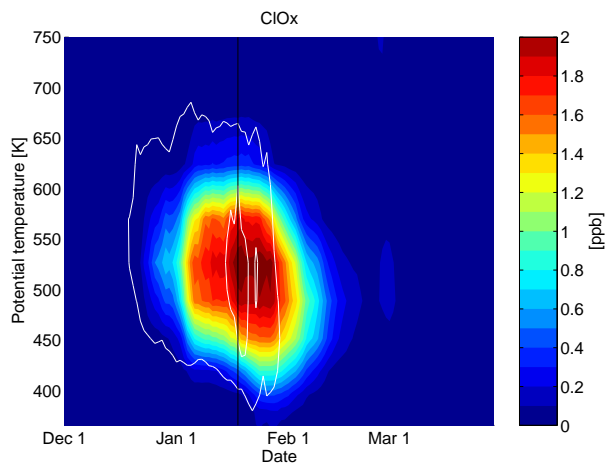


Fig. 1. Vortex-averaged ClO_x in the reference run as a function of model date and potential temperature, averaged over all air parcels inside the vortex boundary according to the Nash criterion (Nash et al., 1996) and over several potential temperature intervals equivalent to the vertical resolution of the model. Before 23 December 2009 and after 26 February 2010, the Nash criterion is not applicable and replaced by a constant value of 68.5° equivalent latitude. White lines show the time periods where the formation of NAT clouds (outer line) and ice clouds (inner line) was possible inside the vortex. The thin black line shows the date of the profiles in Fig. 4.

[Title Page](#)[Abstract](#)[Introduction](#)[Conclusions](#)[References](#)[Tables](#)[Figures](#)[◀](#)[▶](#)[◀](#)[▶](#)[Back](#)[Close](#)[Full Screen / Esc](#)[Printer-friendly Version](#)[Interactive Discussion](#)

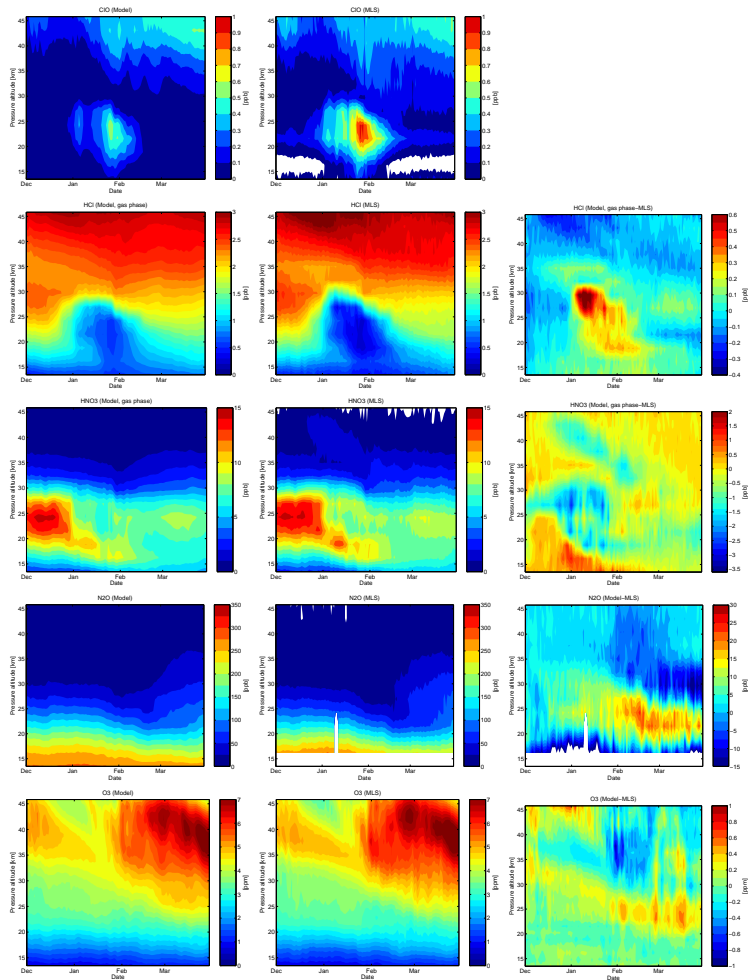


Fig. 2. See caption on next page.

Uncertainties in modeling ozone depletion

I. Wohltmann et al.

Title Page

Abstract Introduction

Conclusions References

Tables Figures

◀ ▶

◀ ▶

Back Close

Full Screen / Esc

Printer-friendly Version

Interactive Discussion



Uncertainties in modeling ozone depletion

I. Wohltmann et al.

Title Page

Abstract

Introduction

Conclusions

References

Tables

Figures

◀

▶

◀

▶

Back

Close

Full Screen / Esc

Printer-friendly Version

Interactive Discussion



Fig. 2. Comparison of vortex averages of several species between the reference run of the model and MLS satellite measurements. Left: Vortex-averaged mixing ratio of the model as a function of model date and altitude, horizontally averaged as in Fig. 1, vertically averaged in pressure layers centered at the MLS retrieval levels. Middle: Same for the MLS measurements. Right: Difference between model and MLS. Top to bottom: ClO, HCl, HNO₃, N₂O, O₃. The difference between model and MLS is not shown for ClO, since a quantitative comparison is meaningless due to the different distribution of local times of observations and model air parcels.

Uncertainties in modeling ozone depletion

I. Wohltmann et al.

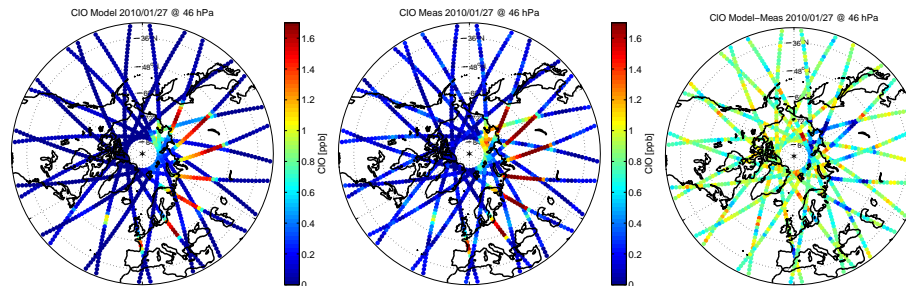


Fig. 3. Modeled (left) and measured (middle) CIO mixing ratios at the MLS layer centered at 46 hPa along the satellite tracks of 27 January. The right panel shows the differences. Backward trajectories starting at the satellite measurements and ending at the time of the last model output before the measurement were calculated. Then, a chemical box model was initialized with the model data and the evolution of the species was calculated forward in time to obtain values to compare with the satellite measurements.

[Title Page](#)[Abstract](#)[Introduction](#)[Conclusions](#)[References](#)[Tables](#)[Figures](#)[◀](#)[▶](#)[◀](#)[▶](#)[Back](#)[Close](#)[Full Screen / Esc](#)[Printer-friendly Version](#)[Interactive Discussion](#)

Uncertainties in modeling ozone depletion

I. Wohltmann et al.

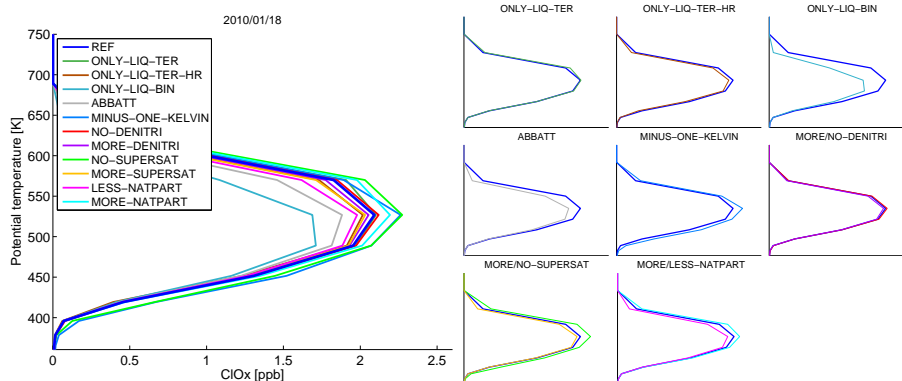


Fig. 4. Vortex-averaged ClO_x for 18 January 2010 as a function of potential temperature for all sensitivity runs and the reference run. Colors indicate the different sensitivity runs. Vortex average as in Fig. 1. The small plots on the right show only one or two sensitivity runs and the reference run at the same time for clarity.

Title Page

Abstract	Introduction
Conclusions	References
Tables	Figures

⏪ ⏩
⏴ ⏵
Back Close

Full Screen / Esc

Printer-friendly Version

Interactive Discussion



Uncertainties in modeling ozone depletion

I. Wohltmann et al.

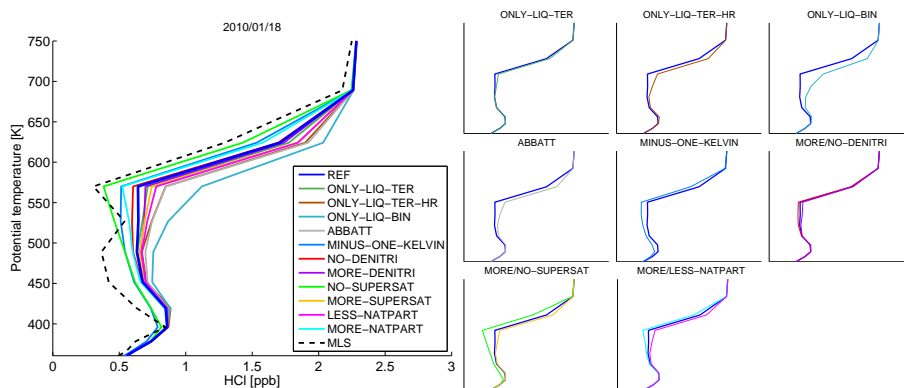


Fig. 5. Vortex-averaged HCl for 18 January 2010 as a function of potential temperature for all sensitivity runs and the reference run. Colors indicate the different sensitivity runs. The black dashed line shows corresponding HCl measurements from MLS. Vortex average as in Fig. 1. The small plots on the right show only one or two sensitivity runs and the reference run at the same time for clarity.

Title Page

Abstract Introduction

Conclusions References

Tables Figures

◀ ▶

◀ ▶

Back Close

Full Screen / Esc

Printer-friendly Version

Interactive Discussion



Uncertainties in modeling ozone depletion

I. Wohltmann et al.

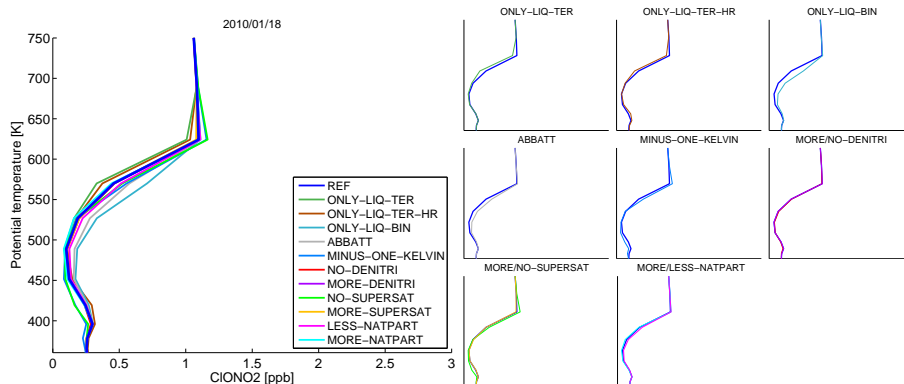


Fig. 6. Vortex-averaged ClONO_2 for 18 January 2010 as a function of potential temperature for all sensitivity runs and the reference run. Colors indicate the different sensitivity runs. Vortex average as in Fig. 1. The small plots on the right show only one or two sensitivity runs and the reference run at the same time for clarity.

Title Page

Abstract Introduction

Conclusions References

Tables Figures

◀ ▶

◀ ▶

Back Close

Full Screen / Esc

Printer-friendly Version

Interactive Discussion



Uncertainties in modeling ozone depletion

I. Wohltmann et al.

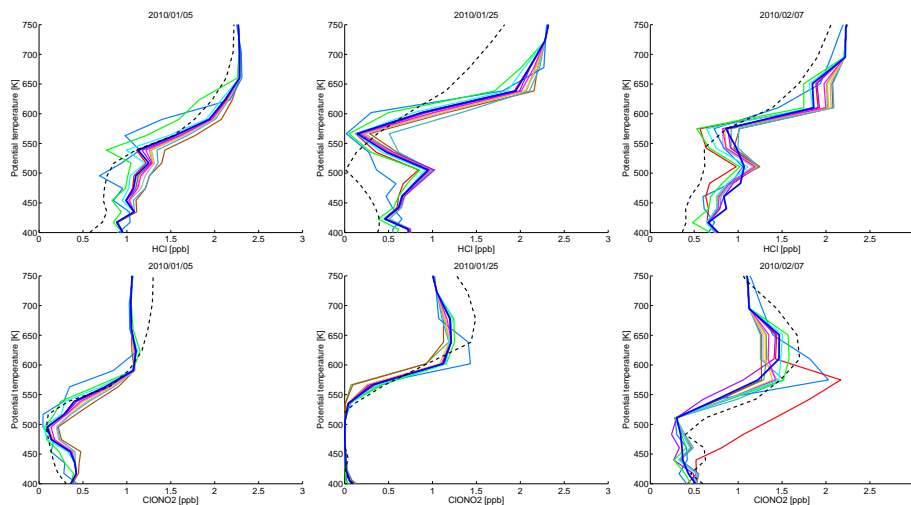


Fig. 7. HCl and ClONO₂ as a function of potential temperature for all sensitivity runs and the reference run for three selected locations in the vortex on different days (5 January at 56.8° N and 15.1° E, 25 January at 65.2° N and 69.4° E, 7 February at 67.4° N and 29.3° E). Colors indicate the different sensitivity runs (see legend in Fig. 5). The black dashed lines show corresponding measurements from ACE-FTS.

[Title Page](#)[Abstract](#)[Introduction](#)[Conclusions](#)[References](#)[Tables](#)[Figures](#)[◀](#)[▶](#)[◀](#)[▶](#)[Back](#)[Close](#)[Full Screen / Esc](#)[Printer-friendly Version](#)[Interactive Discussion](#)

Uncertainties in modeling ozone depletion

I. Wohltmann et al.

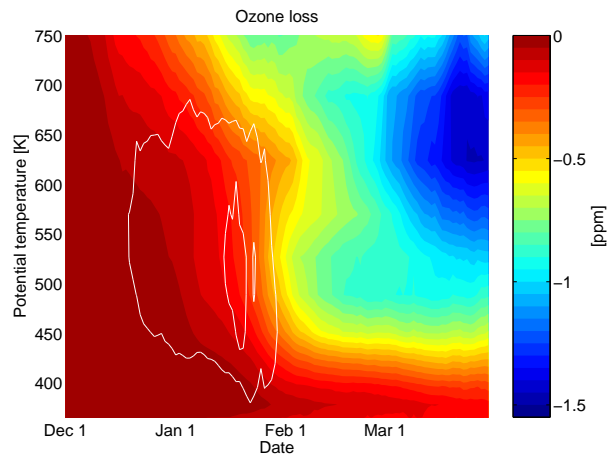


Fig. 8. Vortex-averaged ozone loss for the reference run as a function of model date and potential temperature. Difference between the passive ozone tracer and the modeled ozone averaged as in Fig. 1. The white lines show the time periods where the formation of NAT clouds (outer line) and ice clouds (inner line) was possible inside the vortex.

[Title Page](#)[Abstract](#)[Introduction](#)[Conclusions](#)[References](#)[Tables](#)[Figures](#)[◀](#)[▶](#)[◀](#)[▶](#)[Back](#)[Close](#)[Full Screen / Esc](#)[Printer-friendly Version](#)[Interactive Discussion](#)

Uncertainties in modeling ozone depletion

I. Wohltmann et al.

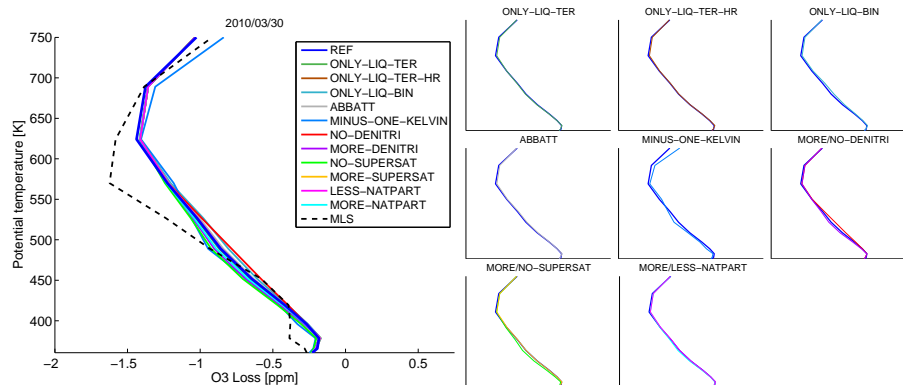


Fig. 9. Vortex-averaged ozone loss for 30 March 2010 as a function of potential temperature for all sensitivity runs and the reference run. Colors indicate the different sensitivity runs. The black dashed line shows the corresponding ozone loss obtained by subtracting MLS ozone measurements from the passive ozone tracer of the model. Vortex average as in Fig. 1. The small plots on the right show only one or two sensitivity runs and the reference run at the same time for clarity.

[Title Page](#)
[Abstract](#)
[Introduction](#)
[Conclusions](#)
[References](#)
[Tables](#)
[Figures](#)
[◀](#)
[▶](#)
[◀](#)
[▶](#)
[Back](#)
[Close](#)
[Full Screen / Esc](#)
[Printer-friendly Version](#)
[Interactive Discussion](#)


Uncertainties in modeling ozone depletion

I. Wohltmann et al.

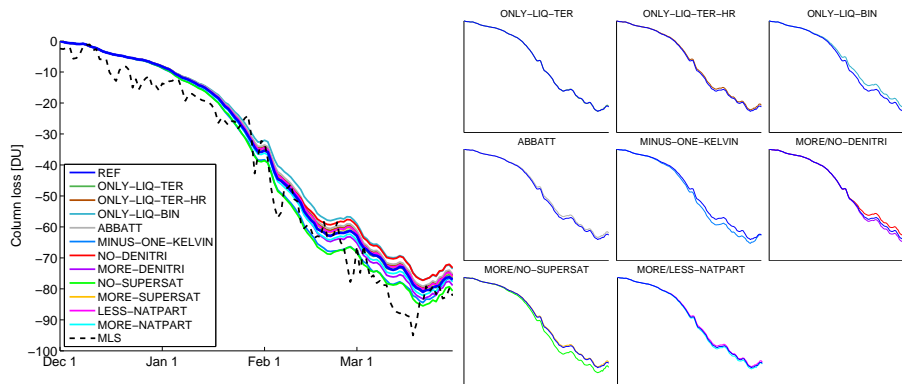


Fig. 10. Vortex-averaged column ozone loss as a function of model date. Colors indicate the different sensitivity runs. The black line shows the column ozone loss obtained by subtracting MLS ozone measurements from the passive ozone tracer of the model. Vortex average as in Fig. 1. The small plots on the right show only one or two sensitivity runs and the reference run at the same time for clarity.

Title Page

Abstract Introduction

Conclusions References

Tables Figures

◀ ▶

◀ ▶

Back Close

Full Screen / Esc

Printer-friendly Version

Interactive Discussion



Uncertainties in modeling ozone depletion

I. Wohltmann et al.

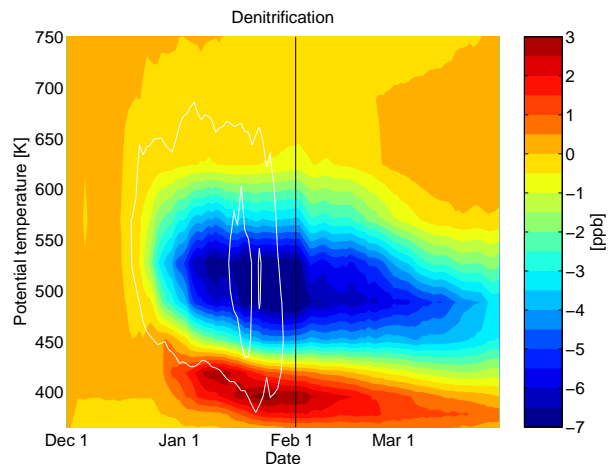


Fig. 11. Vortex-averaged denitrification for the reference run as a function of model date and potential temperature. Difference between the passive NO_y tracer and the modeled NO_y , averaged as in Fig. 1. The thin black line shows the date of the profiles in Figure 12.

[Title Page](#)[Abstract](#)[Introduction](#)[Conclusions](#)[References](#)[Tables](#)[Figures](#)[◀](#)[▶](#)[◀](#)[▶](#)[Back](#)[Close](#)[Full Screen / Esc](#)[Printer-friendly Version](#)[Interactive Discussion](#)

Uncertainties in modeling ozone depletion

I. Wohltmann et al.

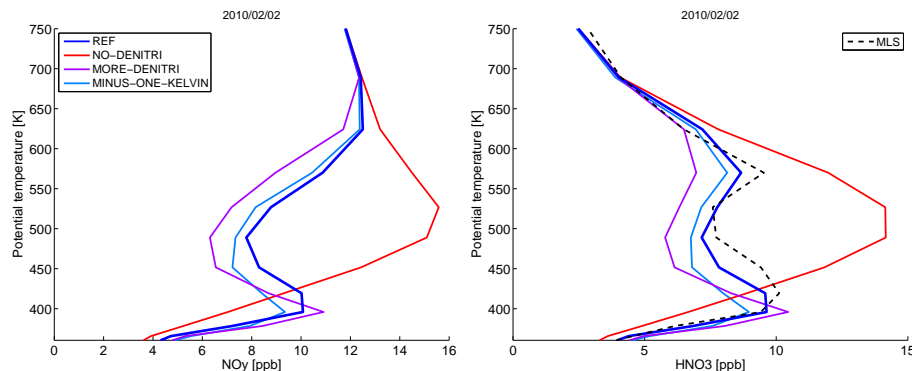


Fig. 12. Vortex-averaged NO_y and HNO_3 for 2 February 2010 as a function of potential temperature for the relevant sensitivity runs (reference run REF, run with no denitrification NO-DENITRI and run with the nucleation rate multiplied by 10 MORE-DENITRI). Colors indicate the different sensitivity runs. The left panel shows the total (solid and gas-phase) NO_y , the red line (NO-DENITRI run) is identical to the passive NO_y tracer. The right panel shows total HNO_3 (identical to gas-phase HNO_3 on this day). The black dashed line shows corresponding HNO_3 measurements from MLS. Vortex average as in Fig. 1.

[Title Page](#)[Abstract](#)[Introduction](#)[Conclusions](#)[References](#)[Tables](#)[Figures](#)[◀](#)[▶](#)[◀](#)[▶](#)[Back](#)[Close](#)[Full Screen / Esc](#)[Printer-friendly Version](#)[Interactive Discussion](#)

Uncertainties in modeling ozone depletion

I. Wohltmann et al.

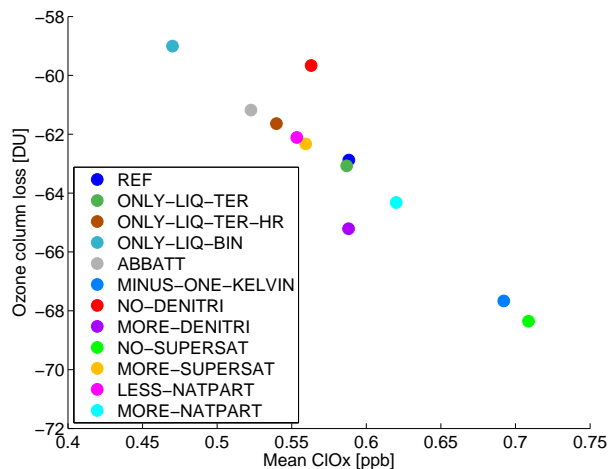


Fig. 13. Extent of chlorine activation versus column ozone loss. Average of vortex mean ClO_x between 15 December and 15 February and 405 to 655 K versus vortex mean column ozone loss on 1 March.

Title Page

Abstract Introduction

Conclusions References

Tables Figures

◀ ▶

◀ ▶

Back Close

Full Screen / Esc

Printer-friendly Version

Interactive Discussion

